

1 **Response to referees of submission of:**

2
3 **The atmospheric impacts of monoterpene ozonolysis on global stabilised Criegee**
4 **intermediate budgets and SO₂ oxidation: experiment, theory and modelling by Newland et**
5 **al., 2017, submitted to ACPD**

6
7

8 **General Response**

9

10 We thank the referees for giving their time to make insightful comments, helping to clarify
11 and further improve our manuscript. All 3 referee's recognise the importance of the results
12 presented, and recommend publication in ACP.

13

14 A couple of significant changes to note are:

15

16 (i) The removal of part of Section 5.2.4, 'Experimental Summary' and all of
17 Section 7, 'Discussion and Atmospheric Implications', as requested by
18 reviewer #3. No information has been lost from the manuscript, these
19 sections were, as pointed out by reviewer #3, somewhat repeating previous
20 sections, a little of Section 7 has been merged into the Conclusions.

21

22 (ii) The use of the IUPAC recommended rate coefficient for the decomposition
23 rate of (CH₃)₂COO, as recommended by R. Chhantyal-Pun in a Comment. This
24 has tended to increase the burden of SCI-B in our global modelling study, and
25 increase the removal of SO₂ by SCI by ~ 20%.

26

27 See the replies to the specific reviewer for further details of these changes.

28

29 Responses to specific points raised by each reviewer are given separately beneath that point.
30 Referees comments are bold and italic, the author's comments are inset in plain type.

31

32 **Anonymous Referee #1**

33 ***First, the authors should clarify the difference between the real atmospheric environment***
34 ***and their chamber. The real atmospheric environment has a range of temperature, relative***
35 ***humidity, and pressure; they should say which temperature, humidity, pressure range can***
36 ***be attained in their chamber.***

37 We agree that we could be clearer that the results are applicable to the atmospheric
38 boundary layer (i.e. surface pressure). This is where the chemistry is important as
39 alkene concentrations are low outside the boundary layer due to their short
40 atmospheric lifetimes. We have clarified this in the abstract by amending the fifth
41 sentence (P2, L2-6) to read:

42 *"We have investigated the removal of SO₂ by SCI formed from the ozonolysis of three*
43 *atmospherically important monoterpenes (α -pinene, β -pinene and limonene) in the*

1 *presence of varying amounts of water vapour in large-scale simulation chamber*
2 *experiments, representative of boundary layer conditions.”*

3 EUPHORE is an outdoor environmental chamber and as such we have no control over
4 the temperature. It is stated that temperature varied between 287 – 302 K across the
5 experiments (p10, I28).

6 We clearly state the relative humidity of each experiment (as is required - the whole
7 point of the experiments is to determine the effect of RH), as well as giving the overall
8 range in the experimental section (p11, I12).

9 ***Second, on page 22, lines 13-16, the authors mention the issues concerning the non-linear***
10 ***results for the limonene results in Figure 2. Can the authors cool the limonene before***
11 ***entering the chamber to decrease the ozonolysis rate? Or can they try an experiment at***
12 ***lower temperatures, to obtain cleaner data for low humidity?***

13 Unfortunately we are unable to perform further experiments at EUPHORE as they
14 were a part of the REACT-SCI campaign in 2013. The possible issue with the non-
15 linearity of the limonene loss is not the reaction rate per se, but more the low volatility
16 of the limonene precursor, meaning that a period of a few minutes is required to add
17 the compound to the chamber. Cooling the sample would only exacerbate this effect.

18 As stated above, EUPHORE is an outdoor environmental chamber and hence we have
19 no control over the chamber temperature.

20 ***Third, cyclohexane is used as an OH scavenger. Is the SCI reaction with cyclohexane slow***
21 ***that it will not interfere with their analysis?***

22 Reaction rates of SCI with alkanes are thought to be very slow. Recent theoretical work
23 (Xu et al., 2017) has calculated reaction rates of CH₂OO with cyclohexane to be 5.7 x
24 10⁻²² cm³ s⁻¹. At 75 ppmv cyclohexane, as employed in our experiments, this would lead
25 to loss rates for CH₂OO to the alkane on the order of 1 x 10⁻¹⁶ s⁻¹, eight orders of
26 magnitude lower than typical loss rates to decomposition or reaction with water.

27

28 ***Small points that can be fixed are as follows:***

29 ***In page 13 lines 11-13, the authors mention that water dimer reaction will be negligible at***
30 ***atmospherically accessible [H₂O]. However, it has already been shown experimentally that***
31 ***for anti-CH₃CHO water vapor reaction, water dimer reaction will dominate the room***
32 ***temperature reaction at a relative humidity (RH) above 30%. (PCCP, 18, 28189-, 2016) On***
33 ***the other hand, the present chamber experiments were done at RH 0.1 to 28%. Therefore,***
34 ***the authors should change this part to “For the analysis of the present chamber results the***
35 ***water dimer reaction can be ignored.”***

1 The referee is right to point out the work of Lin et al. (2016) on *anti*-CH₃CHO + (H₂O)₂.
2 We have altered this paragraph in response to this comment. We have moved the first
3 part of the paragraph to the introduction in response to a comment from referee #2.
4 We now include the following paragraph in the introduction:

5 *"To date, the effects of the water dimer, (H₂O)₂ on SCI removal have only been*
6 *determined experimentally for CH₂OO (Berndt et al., 2014; Chao et al., 2015; Lewis*
7 *et al., 2015; Newland et al., 2015a; Sheps et al., 2017; Liu et al., 2017) and anti-*
8 *CH₃CHO (Lin et al., 2016). Theoretical calculations (Vereecken et al., 2017) have*
9 *predicted the ratio of the SCI + (H₂O)₂ : SCI + H₂O rate constants, k_5/k_3 , of larger, and*
10 *more substituted SCI, to be of a similar order of magnitude as for CH₂OO (i.e. 1.5–2.5*
11 *$\times 10^3$)."*

12 The referee is also right that the dimer reaction will have a negligible impact on the
13 water reaction rates determined in this work because the RH is relatively low and
14 because at the RH where the dimer begins to become a significant loss for *anti*-SCI,
15 almost all of the *anti*-SCI is already being removed by the monomer. Hence there is a
16 negligible effect on the SO₂ loss. The paragraph in Section 2.2 now reads:

17 *"The water dimer reactions of non-CH₂OO SCI are not considered in our analysis. The*
18 *effect of the water dimer reaction with C₁₀ and C₉ SCI (rather than the monomer) is*
19 *expected to be minor at the maximum [H₂O] ($2 \times 10^{17} \text{ cm}^{-3}$) used in these experiments*
20 *(< 30 % RH). Further, with analogy to the syn/anti-CH₃CHO system, for syn-SCI loss*
21 *to the dimer (and monomer) will not become competitive at the highest [H₂O] used*
22 *here; for anti-SCI, the water monomer will already be removing the majority of the*
23 *SCI at the [H₂O] at which the dimer would become a significant loss process, hence*
24 *the dimer reaction is deemed unimportant. For CH₂OO, the reaction rates with water*
25 *and the water dimer have been quantified in recent EUPHORE experimental studies,*
26 *and the values from Newland et al. (2015a) are used in our analysis."*

27
28 ***In Page 21 lines 23-24, they mention the effective rates for the SCI water vapour reaction***
29 ***at RH 75%, 298 K, and discuss results, but their experimental chamber results are up to RH***
30 ***28%, so I am not sure it is relevant to mention the results for such high RH.***

31 We agree with the referee, while the aim of the work is to determine the impact of the
32 SCI under boundary layer conditions, this comment perhaps doesn't belong in the
33 experimental section but instead in a discussion section. We have changed these lines
34 to reflect the experimental conditions from:

35
36 *"SCI-3 is expected to undergo unimolecular reactions at least an order of magnitude*
37 *faster than SCI-4 (Nguyen et al., 2009; Ahrens et al., 2014). The reaction of SCI-3 with*
38 *water is expected to be slow based on the calculations presented in Table 4, with a*
39 *pseudo first order reaction rate of 1.0 s^{-1} at 75 % RH, 298 K, whereas the water reaction*
40 *with SCI-4 is expected to be considerably faster with a pseudo first order reaction rate*
41 *of 240 s^{-1} at 75 % RH, 298 K. This reaction will thus likely be the dominant fate of SCI-4*

1 at typical atmospheric RH. This is in agreement with the observations of Ma and
2 Marston (2008), that show a clear dependence of nopinone formation on RH
3 (presumed to be formed from SCI + H₂O). Fitting Equation E4 to the data determines
4 values of $\gamma^A = 0.41$ and $\gamma^B = 0.59$ (Figure 4).”

5
6 To:

7
8 “SCI-3 is expected to undergo unimolecular reactions at least an order of magnitude
9 faster than SCI-4 (Nguyen et al., 2009; Ahrens et al., 2014). The reaction of SCI-3 with
10 water is expected to be slow based on the calculations presented in Table 4, with a
11 pseudo first order reaction rate of 0.3 s^{-1} at the highest [H₂O] used here, $2 \times 10^{17} \text{ cm}^{-3}$,
12 298 K, whereas the water reaction with SCI-4 is expected to be considerably faster with
13 a pseudo first order reaction rate of 85 s^{-1} at [H₂O] = $2 \times 10^{17} \text{ cm}^{-3}$, 298 K. This reaction
14 would thus be expected to be competitive with reaction with SO₂ for SCI-4 under the
15 experimental conditions employed. This is in agreement with the observations of Ma
16 and Marston (2008), that show a clear dependence of nopinone formation on RH
17 (presumed to be formed from SCI + H₂O). Fitting Equation E4 to the data determines
18 values of $\gamma^A = 0.41$ and $\gamma^B = 0.59$ (Figure 4).”

19 **Anonymous Referee #2**

20 **Provide more information how it was done and what's the accuracy, detection limit etc.**

21 We have added the following information on instrumental precision to the
22 experimental section:

23 “SO₂ and O₃ abundance were measured using conventional fluorescence (reported
24 precision ± 1.0 ppbv) and UV absorption monitors (reported precision ± 4.5 ppbv),
25 respectively;”

26 Experimental procedure is detailed clearly in Section 2.1 (p.10, l.23 – p.11, l.14).

27 **Scavenged the majority of the SCI.” Why the authors did not chose perfect experimental**
28 **conditions for these titration experiments allowing a direct determination of the sCI**
29 **fraction without any further processing of the primary data?**

30 It is impossible to scavenge 100 % of the SCI; rates of decomposition of many of the
31 SCI studied are on the order of hundreds per second. There is a limit to how much SO₂
32 we can safely and practically use in the large EUPHORE chamber (with the lab situated
33 directly below it).

34 **p.17/18 and table 1: Finally stated sCI yields have a quite low range of uncertainty. Does**
35 **the uncertainty really reflect the overall precision of this experimental approach?**

36 We have added a sub-section to Section 2 – Experimental uncertainties which contains
37 the following text:
38

1 *“The uncertainty in k_3/k_2 was calculated by combining the mean relative errors from*
2 *the precision associated with the SO_2 and ozone measurements (given in Section 2.1)*
3 *with the 2σ error and the relative error in φ , using the root of the sum of the squares*
4 *of these four sources of error. The uncertainty in k_d/k_2 was calculated in the same*
5 *way.*

6 *The uncertainty in φ_{min} was calculated by combining the uncertainty in ΔSO_2 and ΔO_3 ,*
7 *as above. The uncertainty in φ was calculated by applying the k_3/k_2 uncertainties and*
8 *combining these with the uncertainties in φ_{min} , using the root of the sum of the*
9 *squares.”*

10 ***Rate coefficients to set their relative values on an absolute scale, Sheps et al., PCCP (2014).***
11 ***Especially by Taatjes et al., Science (2013). Is there a special reason using the Sheps et al.***
12 ***values? What are the consequences if the Taatjes et al. data are used instead of those by***
13 ***Sheps et al.?***

14 The difference between the Sheps and the Taatjes measured rate constants for the
15 anti- $\text{CH}_3\text{CHO} + \text{SO}_2$ reaction is likely owing to differences in the detection techniques
16 used (UV-cavity enhanced absorption spectroscopy vs. Photo-Ionization Mass
17 Spectrometry), with the broadband UV-cavity enhanced absorption
18 technique affording superior sensitivity and selectivity over PIMS (also note that the
19 yield of stabilised anti- CH_3CHO from the $\text{CH}_3\text{CHI} + \text{O}_2$ reaction is only between 10-
20 30% of the total stabilised CH_3CHO yield). Therefore, it was decided to put our
21 chamber relative rate measurements on an absolute basis using
22 the Sheps measurements. However, it is important to point out here that our relative
23 rate measurements can be placed on an absolute basis using new and improved
24 evaluated SO_2 rate constants as new measurements become available.

25
26
27
28

1 **Anonymous Referee #3**

2

3 **Scholarly presentation: The text on monoterpene ozonolysis in the early part of the**
4 **manuscript is a very nice and thorough summary but when read the reader is asking**
5 **himself: 'And what is the outcome of the present paper for this ?' - this is then treated in**
6 **the results section. Maybe some on the contents of the introductory text can be shortened**
7 **and be used when the results are actually presented. That would also compact the paper**
8 **to some extent. Shortening certain sections and avoiding doubling of text appears**
9 **advisable as the manuscript reads kind of lengthy at times. There is the danger to loose the**
10 **reader. The theoretical chemistry section of the paper might be problematic, but I am not**
11 **an expert in this.**

12

13 **Details:**

14 **Page 4, line 4: The population of Cls is formed...pls check sentence.**

15 Changed to, "The population of Cls is formed ..."

16 **p12, l6: This equation looks strangely formatted. Pls check.**

17 We're not sure what looks strange about it, but it will in any case be formatted to the
18 ACP style during typesetting.

19 **p13-15 - 15: I feel this is partly repeating material already given in the introductory**
20 **overview. That should be avoided. Please check and discuss the state-of-the art regarding**
21 **the water reaction, the roles of the water dimer and the difference of syn- and anti-**
22 **conformers once in the manuscript and then work with internal referencing.**

23 We have moved the 'literature review' part of this paragraph to the introduction and
24 included all up to date references. This section now reads:

25 "To date, the effects of the water dimer, (H₂O)₂ on SCI removal have only been
26 determined experimentally for CH₂OO (Berndt et al., 2014; Chao et al., 2015; Lewis
27 et al., 2015; Newland et al., 2015a; Sheps et al., 2017; Liu et al., 2017) and anti-
28 CH₃CHOO (Lin et al., 2016). Theoretical calculations (Vereecken et al., 2017) have
29 predicted the ratio of the SCI + (H₂O)₂ : SCI + H₂O rate constants, k₅/k₃, of larger, and
30 more substituted SCI, to be of a similar order of magnitude as for CH₂OO (i.e. 1.5–2.5
31 × 10³)."

32 **p16: If it has been shown, that post-CCSD(T) calculations are needed but these cannot be**
33 **performed for technical reason, what is then the use of this? It is difficult to judge how**
34 **valid such calculations could be. Certain journals do not accept theoretical chemistry**
35 **calculation not being performed with the best available techniques. The authors should**
36 **deal with this. Maybe it is better to outsource this part and do the bigger calculations**
37 **separately.**

1 Like experimental measurements, all theoretical predictions are subject to an
2 uncertainty margin, where one aims to reduce the uncertainty by applying the highest
3 possible levels of theory. The methodology used in this work is generally considered
4 high-level and reliable, and the data presented here required well over half a million
5 cpu core hours (>>50 years), and include CCSD(T) calculations with over 1000 basis
6 functions. It is doubtful that any journal would consider these calculations not state-
7 of-the-art for the molecules studied. Going beyond these methodologies is not
8 obvious, and it is not a matter of outsourcing post-CCSD(T) calculations, but rather the
9 question whether anyone is able to do them at all with current computational
10 resources, and can/wants to afford the cost, especially as the empirical corrections
11 described in Vereecken et al. 2017 are expected to recover a large part of the bias on
12 the barrier height. Further improvement could perhaps be made by the kinetic analysis
13 but this, too, requires significant additional computational resources.

14
15 As shown in Vereecken et al. 2017, the final rate coefficient predictions for
16 unimolecular reactions are expected to be accurate within a factor of 5. For the Cl +
17 H₂O reaction, rate predictions are estimated to be accurate within an order of
18 magnitude. While it would be useful to further reduce the uncertainty on these
19 predictions, they are already sufficiently accurate to have useful predictive value, and
20 the computational cost of reducing the uncertainty may suffer from diminishing
21 returns.

22
23 The use of these predictions is that we now have two studies with very different
24 methodologies, experimental and theoretical, which agree quantitatively within the
25 respective uncertainties, suggesting that the conclusions presented in the paper are
26 reliable. Furthermore, the theoretical data allows one to identify the molecular
27 identity of the Cl groups used in the experimental analysis; this data is not readily
28 available otherwise.

29 We have changed the first paragraph of Section 3 to read:

30 *“The rovibrational characteristics of all conformers of the Cl formed from α -pinene and*
31 *β -pinene, the transition states for their unimolecular reaction, and for their reaction*
32 *with H₂O, were characterized quantum chemically, first using the M06-2X/cc-pVDZ*
33 *level of theory, and subsequently refined at the M06-2X/aug-cc-pVTZ level. To obtain*
34 *the most accurate barrier heights for reaction, it has been shown (Berndt et al., 2015;*
35 *Chhantyal-Pun et al., 2017; Fang et al., 2016a, 2016b; Long et al., 2016; Nguyen et al.,*
36 *2015) that post-CCSD(T) calculations are necessary. Performing such calculations for*
37 *the SCI discussed in this paper, with up to 14 non-hydrogen atoms, is well outside our*
38 *computational resources. Instead, we base our predictions on high-level CCSD(T)/aug-*
39 *cc-pVTZ single point energy calculations, performed for the reactions of nopinone*
40 *oxides and the most relevant subset of pinonaldehyde oxides. These data are reliable*
41 *for relative rate estimates, but it remains useful to further improve the absolute barrier*
42 *height predictions, as described by Vereecken et al. (2017) based on a data set with a*
43 *large number of systematic calculations on smaller Cl, allowing empirical corrections*
44 *to estimate the post-CCSD(T) barrier heights. Briefly, they compare rate coefficient*

1 *calculations against available harmonized experimental and very-high level theoretical*
2 *kinetic rate predictions, and adjusts the barrier heights by 0.4 to 2.6 kcal mol⁻¹*
3 *(depending on the base methodology and the reaction type) to obtain best agreement*
4 *with these benchmark results.”*

5

6 ***p18,l29: Pls check sentence***

7 Checked.

8 ***p23, Is that section 5.2.4. really needed? I think it should be skipped in order to streamline***
9 ***the whole paper.***

10 We agree that much of this section is repeated in the conclusions and that parts of the
11 section could be removed to shorten the paper, but also feel that it is useful to provide
12 a summary of the experimental numbers from the previous sections. As such, we have
13 significantly shortened this section, removing the first 15 lines and the final paragraph.

14 ***p24, section 5.3: See general comment on this. Is it necessary to give all the structural data***
15 ***in the SI?***

16 It is not clear whether the referee is requesting more structural data in the main
17 manuscript, or less in the SI. If it is the latter, then we would suggest that this is exactly
18 what the SI is for. We would hope that the information will be useful for those looking
19 to further understand the theoretical work.

20 ***p 26, Why is section 6 separate from the 'results' section - these are also results, so it might***
21 ***be sensible to make this a sub-point of the results section 5 rather than a new section 6***

22 We agree that the current grouping of the experimental and theoretical results, but
23 separation of the modelling is somewhat illogical. The three separate techniques:
24 experiment, theory, and modelling are now placed in separate sections. This seems to
25 us a logical and useful way of setting out the paper. In order to clarify the differences
26 between these sections we have renamed Section 5, **Experimental Results**.
27 **Theoretical results and comparison to experiments** is now Section 6. And **Global**
28 **modeling study** is now Section 7.

29 ***p29, l 14: Oceanic MT emissions are expected to be small compared to the continental***
30 ***ones.***

31 This may be the case, but we clearly reference two studies which provide values for
32 oceanic MT emissions and then discuss the implication of these studies with reference
33 to our work.

34 ***p30, sections 7 & 8: Maybe these sections can be combined.***

1 We agree with the referee, Section 7 has been removed and the following sentence
2 has been added to the conclusion (with reference to using a 2-species system for
3 modelling SCI chemistry).

4 *“Moreover such an approach is required to accurately predict SCI concentrations, which*
5 *will be underestimated if a simple average of the properties of the two different SCI*
6 *classes is used.”*

7

8

1 **Comment – Rabi Chhantyal-Pun**

2 ***Please could the authors clarify why a value of 819 (± 190) s⁻¹ is being used for (CH₃)₂COO***
3 ***unimolecular reaction rate coefficient? The recent IUPAC task group on atmospheric***
4 ***chemical kinetic data evaluation's preferred value is 397 s⁻¹ at 298 K. Is the author's global***
5 ***modelling study affected if more accurate rate coefficients are used?***

6 The value originally used for the (CH₃)₂COO decomposition rate (819 s⁻¹) comes from
7 ozonolysis experiments (Newland et al., 2015) that used the same experimental
8 conditions as those used in the monoterpene experiments reported in the manuscript.
9 The relative rate from Newland et al. (2015) was scaled to the k((CH₃)₂COO+SO₂) rate
10 determined by Huang et al. (2015). This values lies within the uncertainty limits of the
11 recommended IUPAC value.

12 However, we agree with R. Chhantyal-Pun that the modelling should be done with the
13 IUPAC recommended value (which was not available when the modelling was
14 originally done!). We have repeated the global modeling using the temperature
15 dependent decomposition value from IUPAC ([http://iupac.pole-ether.fr/htdocs/datasheets/pdf/CGI_14_\(CH3\)2COO+M.pdf](http://iupac.pole-ether.fr/htdocs/datasheets/pdf/CGI_14_(CH3)2COO+M.pdf)) and will include this
16 revised model output in the final manuscript.
17

18 As expected, using this slower unimolecular rate increases the concentrations of the
19 SCI-B from ocimene and myrcene, for which the acetone oxide kinetics are used. These
20 increased concentrations lead to an increased relative importance of these SCI
21 compared to other SCI and increased removal of SO₂.

22 The relative contributions of myrcene and ocimene to total [SCI-B] increase from 1.2
23 % and 5.4 % to 2.7 % and 11% respectively, with commensurate decreases in the
24 relative contributions of the other monoterpenes. Peak annually averaged [SCI] (in the
25 tropics) increases from 1.2 × 10⁴ cm⁻³ to 1.4 × 10⁴ cm⁻³.

26 The contribution of SCI to annual gas phase SO₂ oxidation in the terrestrial tropics
27 increases from 1.1 % – 1.2 %. Globally, the annual contribution of SCI to gas phase SO₂
28 oxidation increases from 0.5 % to 0.7 %, and the total annual SO₂ removal increases
29 from 6.8 to 8.1 Gg.

30 All relevant values have been updated throughout the manuscript. The modelling
31 using the Blitz updated k(SO₂+OH) rate constant in the SI has also been updated.
32

33

34

35

1 **The atmospheric impacts of monoterpene ozonolysis on**
2 **global stabilised Criegee intermediate budgets and SO₂**
3 **oxidation: experiment, theory and modelling**

4
5 **Mike J. Newland^{1,3}, Andrew R. Rickard^{2,3}, Tomás Sherwen³, Mathew J. Evans^{2,3},**
6 **Luc Vereecken^{4,5}, Amalia Muñoz⁶, Milagros Ródenas⁶, William J. Bloss¹**

7 [1]{University of Birmingham, School of Geography, Earth and Environmental Sciences,
8 Birmingham, UK}

9 [2]{National Centre for Atmospheric Science (NCAS), University of York, York, UK}

10 [3]{Wolfson Atmospheric Chemistry Laboratories, Department of Chemistry, University of
11 York, York, UK}

12 [4]{Max Planck Institute for Chemistry, Atmospheric Sciences, Hahn-Meitner-Weg 1, Mainz,
13 Germany}

14 [5]{Institute for Energy and Climate Research, Forschungszentrum Jülich GmbH, Jülich,
15 Germany}

16 [6]{Fundación CEAM, EUPHORE Laboratories, Avda/Charles R. Darwin 14. Parque
17 Tecnológico, Valencia, Spain}

18 Correspondence to: M. J. Newland (mike.newland@york.ac.uk)

19 A. R. Rickard (andrew.rickard@york.ac.uk)

20

21 **Abstract**

22 The gas-phase reaction of alkenes with ozone is known to produce stabilised Criegee
23 intermediates (SCIs). These biradical/zwitterionic species have the potential to act as
24 atmospheric oxidants for trace pollutants such as SO₂, enhancing the formation of sulfate
25 aerosol with impacts on air quality and health, radiative transfer and climate. However, the
26 importance of this chemistry is uncertain as a consequence of limited understanding of the
27 abundance and atmospheric fate of SCIs. In this work we apply experimental, theoretical and
28 numerical modelling methods to quantify the atmospheric impacts, abundance, and fate, of the

1 structurally diverse SCIs derived from the ozonolysis of monoterpenes, the second most
2 abundant group of unsaturated hydrocarbons in the atmosphere. We have investigated the
3 removal of SO₂ by SCI formed from the ozonolysis of three [atmospherically important](#)
4 monoterpenes (α -pinene, β -pinene and limonene) in the presence of varying amounts of water
5 vapour in large-scale simulation chamber experiments, [representative of boundary layer](#)
6 [conditions](#). The SO₂ removal displays a clear dependence on water vapour concentration, but
7 this dependence is not linear across the range of [H₂O] explored. At low [H₂O] a strong
8 dependence of SO₂ removal on [H₂O] is observed, while at higher [H₂O] this dependence
9 becomes much weaker. This is interpreted as being caused by the production of a variety of
10 structurally (and hence chemically) different SCI in each of the systems studied, each
11 displaying different rates of reaction with water and of unimolecular
12 rearrangement/decomposition. The determined rate constants, $k(\text{SCI}+\text{H}_2\text{O})$, for those SCI that
13 react primarily with H₂O range from $4 - 310 \times 10^{-15} \text{ cm}^3 \text{ s}^{-1}$. For those SCI that predominantly
14 react unimolecularly, determined rates range from $130 - 240 \text{ s}^{-1}$. These values are in line with
15 previous results for the (analogous) stereo-specific SCI system of *syn/anti*-CH₃CHOO. The
16 experimental results are interpreted through theoretical studies of the SCI unimolecular
17 reactions and bimolecular reactions with H₂O, characterised for α -pinene and β -pinene at the
18 M06-2X/aug-cc-pVTZ level of theory. The theoretically derived rates agree with the
19 experimental results within the uncertainties. A global modelling study, applying the
20 experimental results within the GEOS-Chem chemical transport model, suggests that [> 97 %](#)
21 of the total monoterpene derived global SCI burden is comprised of SCI whose structure
22 determines that they react slowly with water, and whose atmospheric fate is dominated by
23 unimolecular reactions. Seasonally averaged boundary layer concentrations of monoterpene-
24 derived SCI reach up to $1.4 \times 10^4 \text{ cm}^{-3}$ in regions of elevated monoterpene emissions in the
25 tropics. Reactions of monoterpene derived SCI with SO₂ account for < 1 % globally but may
26 account for up to [60 %](#) of the gas-phase SO₂ removal over areas of tropical forests, with
27 significant localised impacts on the formation of sulfate aerosol, and hence the lifetime and
28 distribution of SO₂.

Deleted: β -

Deleted: .

Deleted: 98

Deleted: 2

Deleted: 50

30 1 Introduction

31 Chemical oxidation processes in the atmosphere exert a major influence on atmospheric
32 composition, leading to the removal of primary emitted species, and the formation of secondary

1 products. In many cases either the emitted species or their oxidation products negatively impact
2 air quality and climate (e.g. ozone, which is also a potent greenhouse gas). These reactions can
3 also transform gas-phase species to the condensed phase, forming secondary aerosol that again
4 can be harmful to health and can both directly and indirectly influence radiative transfer and
5 hence climate (e.g. SO₂ oxidation leading to the formation of sulfate aerosol).

6 Tropospheric gas-phase oxidants include the OH radical, ozone, the NO₃ radical, and halogen
7 atoms. Stabilised Criegee intermediates (SCIs), or carbonyl oxides, have been identified as
8 another potentially important oxidant in the troposphere (e.g. Cox and Penkett, 1971;
9 Mauldin et al., 2012). SCIs are thought to be formed in the atmosphere predominantly from
10 the reaction of ozone with unsaturated hydrocarbons, though other processes may be
11 important under certain conditions, e.g. alkyl iodide photolysis (Gravestock et al., 2010),
12 dissociation of the DMSO peroxy radical (Asatryan and Bozzelli, 2008). Laboratory
13 experiments and theoretical calculations have shown SCI to oxidise SO₂ (e.g. Cox and
14 Penkett, 1971; Welz et al., 2012; Taatjes et al., 2013), organic (Welz et al., 2014) and
15 inorganic (Foreman et al., 2016) acids (Vereecken et al., 2017), and a number of other
16 important trace gases found in the atmosphere, as well as forming adducts with NO₂
17 (Taatjes et al., 2014; Vereecken et al., 2017; Caravan et al., 2017). Measurements in a
18 boreal forest (Mauldin et al., 2012) and at a coastal site (Berresheim et al., 2014) have both
19 identified a ‘missing’ process (in addition to reaction with OH) oxidising SO₂ to H₂SO₄,
20 potentially arising from SCI reactions.

21 Here, we present results from a series of experimental studies into SCI formation and reactions,
22 carried out under atmospheric boundary layer conditions in the European Photochemical
23 Reactor facility (EUPHORE), Valencia, Spain. We examine the ozonolysis of three
24 monoterpenes with very different structures (and hence reactivities with OH and ozone): α -
25 pinene (with an endocyclic double bond), β -pinene (with an exocyclic double bond) and
26 limonene (with both an endo and exo cyclic double bond). We observe the removal of SO₂ in
27 the presence of each alkene-ozone system as a function of water vapour concentration. This
28 allows us to derive relative SCI kinetics for reaction with H₂O, SO₂, and unimolecular
29 decomposition. Further, we calculate absolute unimolecular rates and bimolecular reaction rates
30 with H₂O for all α -pinene and β -pinene derived SCI at the M06-2X/aug-cc-pVTZ level of
31 theory. A global modelling study, using the GEOS-Chem global chemical transport model, is

1 performed to assess global and regional impacts of the chemical kinetics of monoterpene SCI
2 determined in this study.

3 1.1 Stabilised Criegee Intermediate Kinetics

4 Ozonolysis of an unsaturated hydrocarbon produces a primary ozonide that rapidly
5 decomposes to yield pairs of Criegee intermediates (CIs) and carbonyls (Johnson and
6 Marston 2008). The population of CIs are formed with a broad internal energy distribution
7 giving both chemically activated and stabilised forms. Chemically activated CIs may
8 undergo collisional stabilisation to an SCI, unimolecular decomposition or isomerisation.
9 SCIs can have sufficiently long lifetimes to undergo bimolecular reactions (Scheme 1).

10 The predominant atmospheric fate for the simplest SCI, CH₂OO, is reaction with water
11 vapour (likely with the dimer ((H₂O)₂) (e.g. Berndt et al., 2014; Newland et al., 2015a;
12 Chao et al., 2015; Lewis et al., 2015; Lin et al., 2016a). For larger SCI, both experimental
13 (Taatjes et al., 2013; Sheps et al., 2014; Newland et al., 2015a; Huang et al., 2015) and
14 theoretical (Kuwata et al., 2010; Anglada et al., 2011; Anglada and Sole, 2016, Vereecken
15 et al., 2017) studies have shown that their kinetics, in particular reaction with water, are
16 highly structure dependent. The significant double bond character exhibited in the
17 zwitterionic configurations of mono-substituted SCI leads to two distinct chemical forms:
18 *syn*-SCI (*i.e.* those where an alkyl-substituent group is on the same side as the terminal
19 oxygen of the carbonyl oxide moiety), and *anti*-SCI (*i.e.* with the terminal oxygen of the
20 carbonyl oxide moiety on the same side as a hydrogen group). The two conformers of
21 CH₃CHOO, which are both mono-substituted, display these properties. This difference in
22 conformer reactivities has been predicted theoretically (Ryzhkov and Ariya, 2004, Kuwata
23 et al., 2010; Anglada et al., 2011; Lin et al., 2016a) and was subsequently confirmed
24 experimentally (Taatjes et al., 2013; Sheps et al., 2014) for the two CH₃CHOO conformers.
25 The significantly faster reaction of *anti*-CH₃CHOO with water is driven by the higher
26 potential energy of this isomer, while more stable SCI, with a methyl group in *syn*-position,
27 such as *syn*-CH₃CHOO or (CH₃)₂COO, react orders of magnitude more slowly with water.

28 To date, the effects of the water dimer, (H₂O)₂, on SCI removal have only been determined
29 experimentally for CH₂OO (Berndt et al., 2014; Chao et al., 2015; Lewis et al., 2015;
30 Newland et al., 2015a; Sheps et al., 2017; Liu et al., 2017) and *anti*-CH₃CHOO (Lin et al.,
31 2016b). Theoretical calculations (Vereecken et al., 2017) have predicted the ratio of the SCI +

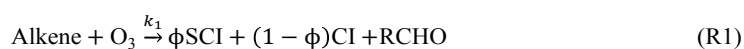
Deleted: 2016

Deleted: 2016

Moved (insertion) [1]

1 [\(H₂O\)₂ : SCI + H₂O rate constants, \$k_2/k_3\$, of larger, and more substituted SCI, to be of a similar](#)
2 [order of magnitude as for CH₂OO \(i.e. \$1.5-2.5 \times 10^3\$ \).](#)

3 SCI can also undergo unimolecular isomerisation/decomposition in competition with
4 bimolecular reactions. This is likely to be a significant atmospheric sink for *syn*-SCI because
5 of their slow reaction with water vapour (e.g. Huang et al., 2015). Unimolecular reactions of
6 *syn*-CI/SCI are dominated by a 1,4-H-shift, forming a vinyl hydroperoxide (VHP) intermediate
7 (Niki et al., 1987; Rickard et al., 1999; Martinez and Herron, 1987; Johnson and Marston, 2008;
8 Kidwell et al., 2016). Decomposition of the VHP formed in this process is an important non-
9 photolytic source of OH, HO₂, and RO₂ in the atmosphere (Niki et al., 1987; Alam et al.,
10 2013; Kidwell et al., 2016), which can also lead to secondary organic aerosol formation
11 (Ehn et al., 2014). Unimolecular reactions of the *anti*-CI/SCI are thought to be dominated
12 by a 1,3-ring closure, the “acid/ester channel”, in which the CI/SCI decomposes, through
13 a rearrangement to a dioxirane intermediate, producing a range of daughter products and
14 contributing to the observed overall HO_x radical yield (Kroll et al., 2002; Johnson and
15 Marston, 2008; Alam et al., 2013).



22 Decomposition of the simplest SCI, CH₂OO, is slow ($< 10 \text{ s}^{-1}$) and is not likely to be an
23 important sink in the troposphere (e.g. Newland et al., 2015a; Chhantyal-Pun et al., 2015). This
24 decomposition occurs primarily via rearrangement through a ‘hot’ acid species, which
25 represents the lowest accessible decomposition channel (Gutbrod et al., 1996; Alam et al., 2011;
26 Chen et al., 2016). However, recently determined unimolecular reaction rates of larger *syn*-SCI
27 are considerably faster. Newland et al. (2015a) reported unimolecular reaction rate constants
28 for *syn*-CH₃CHOO of $348 (\pm 332) \text{ s}^{-1}$ and for (CH₃)₂COO of $819 (\pm 190) \text{ s}^{-1}$ (assuming $k(\text{syn-}$
29 $\text{CH}_3\text{CHOO} + \text{SO}_2) = 2.9 \times 10^{-11} \text{ cm}^3 \text{ s}^{-1}$ (Sheps et al., 2014) and $k((\text{CH}_3)_2\text{COO} + \text{SO}_2) = 1.3 \times 10^{-11}$

1 $10^3 \text{ cm}^3 \text{ s}^{-1}$ (Huang et al., 2015), respectively). Smith et al. (2016) measured the unimolecular
2 decomposition rate of $(\text{CH}_3)_2\text{COO}$ to be $269 (\pm 82) \text{ s}^{-1}$ at 283 K increasing to $916 (\pm 56) \text{ s}^{-1}$ at
3 323 K, suggesting the rate to be fast and highly temperature dependent. Novelli et al. (2014),
4 estimated a significantly slower decomposition rate for *syn*- CH_3CHOO of $20 (3\text{-}30) \text{ s}^{-1}$ from
5 direct observations of OH formation, while Fenske et al. (2000), estimated the decomposition
6 rate of CH_3CHOO (i.e. a mix of *syn* and *anti* conformers) produced from ozonolysis of *trans*-
7 but-2-ene to be 76 s^{-1} (accurate to within a factor of three).

8

9 **1.2 Monoterpene Ozonolysis**

10 Monoterpenes are volatile organic compounds (VOCs) with the general formula $\text{C}_{10}\text{H}_{16}$, which
11 are emitted by a wide range of vegetation, particularly from boreal forests. Total global
12 monoterpene emissions are estimated to be $95 (\pm 3) \text{ Tg yr}^{-1}$ (Sindelarova et al., 2014) - roughly
13 13 % of total non-methane biogenic VOC emissions. Monoterpene emissions are dominated by
14 α -pinene, which accounts for roughly 34 % of the total global emissions, while β -pinene and
15 limonene account for 17 % and 9 % respectively (Sindelarova et al., 2014). Monoterpenes
16 (mainly α -pinene and limonene) are also present in indoor environments, in significant amounts
17 where cleaning products and air fresheners are in routine use (on the order of 100s of ppbv)
18 (e.g. Singer et al., (2006); Sarwar and Corsi, (2007)), where their ozonolysis products can affect
19 indoor chemistry and health (e.g. Rossignol et al., (2013); Shallcross et al., (2014)).

20 Monoterpenes are highly reactive due to the presence of (often multiple) double bonds. The
21 oxidation of monoterpenes yields a wide range of multi-functional gas-phase and aerosol
22 products. This process can be initiated by OH and NO_3 radicals or by O_3 , with ozonolysis
23 having been shown to be particularly efficient at generating low volatility products that can
24 form SOA, even in the absence of sulfuric acid (e.g. Ehn et al., 2014; Kirkby et al., 2016). These
25 highly oxygenated secondary products have received considerable attention in recent years
26 because of their role in affecting the climate through absorption and scattering of solar radiation
27 (the direct aerosol effect). They can also increase cloud condensation nuclei concentrations,
28 which can change cloud properties and lifetimes (the indirect aerosol effect). They have also
29 been shown to have a wide range of deleterious effects on human health (e.g. Pöschl and
30 Shiraiwa, 2015).

31 The ozonolysis reaction for monoterpenes is expected to follow a similar initial process to that

1 of smaller alkenes, with cyclo-addition at a double bond giving a primary ozonide (POZ),
2 followed by rapid decomposition of the POZ to yield a CI and a carbonyl (Scheme 1).
3 Stabilisation of the large POZs formed in monoterpene ozonolysis is expected to be
4 negligible (Nguyen et al., 2009). However, a major difference in ozonolysis at endocyclic bonds
5 is that, on decomposition of the POZ, the carbonyl oxide and carbonyl moieties are tethered as
6 part of the same molecule, providing the potential for further interaction of the two. These can
7 react together to form secondary ozonides (SOZ), which may be stable for several hours (Beck
8 et al., 2011). However, while this has been shown to be potentially the major fate in the
9 atmosphere for SCI derived from sesquiterpenes (C₁₅H₂₄) (e.g. Nguyen et al., 2009b; Beck et
10 al., 2011; Yao et al., 2014), formation of SOZ is predicted to be small for monoterpene derived
11 SCI because of the high ring strain caused by the tight cyclisation (e.g. Nguyen et al., 2009b).
12 Chuong et al. (2004) predicted formation of a SOZ to become the dominant atmospheric fate
13 for SCI formed in the ozonolysis of endo-cyclic alkenes with a carbon number between 8 and
14 15, while Vereecken and Francisco (2012) suggested that internal SOZ formation is likely to
15 be limited to product rings containing six or more carbons due to ring strain.

16 No studies have yet directly determined the reaction rates of the large SCI produced from
17 monoterpene ozonolysis with SO₂ (or any other trace gases). This is owing to the complexities
18 of synthesizing and measuring large SCI. However, Ahrens et al. (2014) concluded that the
19 reaction of the C9-SCI formed in β-pinene ozonolysis with SO₂ is as fast as that determined by
20 Welz et al. (2012) and Taatjes et al. (2013) for CH₂OO and CH₃CHOO respectively (ca. 4 ×
21 10⁻¹¹ cm³ s⁻¹) by fitting to the decay of SO₂ in the presence of the ozonolysis reaction. Mauldin
22 et al. (2012) calculated significantly slower reaction rates for an additional oxidant (assumed to
23 be SCI) derived from α-pinene and limonene ozonolysis, with *k*(SCI+SO₂) determined to be 6
24 × 10⁻¹³ cm³ s⁻¹ and 8 × 10⁻¹³ cm³ s⁻¹ for α-pinene and limonene derived SCI respectively.
25 However, it seems likely that the rates calculated by Mauldin et al. (2012) may be substantially
26 underestimated due to the assumption of a very long SCI lifetime (0.2 s) in experiments that
27 were performed at 50 % RH. The calculated rates scale linearly with SCI lifetime and based on
28 reaction rates of smaller SCI with H₂O (reported since the Mauldin et al. work, e.g. Taatjes et
29 al., 2013) it seems likely that the lifetime of the SCI in their experiments would have been more
30 like 0.1 – 2 × 10⁻² s, increasing the calculated rate constants by more than an order of magnitude,
31 bringing them into much closer agreement with the rates reported by Ahrens et al. (2014).

32 Unimolecular reactions of the monoterpene SCI are expected to proceed rapidly through the
33 VHP route if a hydrogen is available for a 1,4 H-shift. Those SCI that cannot undergo this

1 rearrangement may undergo unimolecular reactions via the formation of the dioxirane
2 intermediate, but this is expected to be a much slower process (Nguyen et al., 2009). In contrast
3 to smaller SCI, it has been observed experimentally, and predicted theoretically, that the VHP
4 route will mainly lead to rearrangement to an acid (also yielding an OH radical) rather than
5 decomposition of the molecule (e.g. Ma et al., 2008, Ma and Marston, 2008). As for the smaller
6 alkenes, monoterpene ozonolysis has been shown to be a source of HO_x (e.g. Paulson et al.,
7 1997; Alam et al., 2013), predominantly via the VHP rearrangement. The MCMv3.3.1 (Jenkin
8 et al., 2015) applies OH yields of 0.80, 0.35 and 0.87 for α -pinene, β -pinene and limonene
9 respectively.

10 1.2.1 α -pinene derived SCI

11 Decomposition of the α -pinene POZ yields four different C₁₀ Criegee intermediates (Scheme
12 2: CI-1a, 1b, 2a, 2b), with the carbonyl oxide moiety at one end and a carbonyl group at the
13 other. Here, CI-1 is a mono-substituted CI for which both *syn* (1a) and *anti* (1b) conformers
14 exist, while the other, CI-2, is di-substituted, for which two *syn*-conformers (2a and 2b) exist.
15 Ma et al. (2008) infer a relative yield of 50 % for the two basic CI formed, based on the
16 observation that nopinonic acid yields from the ozonolysis of α -pinene and an enone, which
17 upon ozonolysis yields CI-1, are almost indistinguishable.

18 The total SCI yield from α -pinene was determined to be 0.15 (\pm 0.07) by Sipilä et al. (2014) in
19 indirect experiments measuring the production of H₂SO₄ from SO₂ oxidation in the α -pinene
20 ozonolysis system. Drozd and Donahue (2011) also determined a total SCI yield of about 0.15
21 at 740 Torr, from measuring the loss of hydrofluoroacetone in ozonolysis experiments in a high
22 pressure flow system. The MCMv3.3.1 (Jenkin et al., 1997; Saunders et al., 2003; Jenkin et al.,
23 2015) applies a value of 0.20 based on stabilisation of only the mono-substituted CI-1.

24 1.2.2 β -pinene derived SCI

25 β -pinene ozonolysis yields two distinct conformers of the nopinone C₉-CI (Scheme 3: CI-3 and
26 CI-4), which differ in orientation of the carbonyl oxide group, and CH₂OO. CI-3 and CI-4 are
27 formed in roughly equal proportions with very little inter-conversion between the two (Nguyen
28 et al., 2009). The difference in the chemical behaviour of CI-3 and CI-4, which were often not
29 distinguished in earlier studies, arises from the inability of the carbon attached to the four-
30 membered ring to undergo the 1,4-H-shift that allows unimolecular decomposition via the VHP
31 channel. This was noted in Rickard et al. (1999) as being a reason for the considerably lower

1 OH yield (obtained via the VHP route) from β -pinene ozonolysis compared to that of α -pinene.
2 This difference leads to contrasting unimolecular decomposition rates for the two CI, with
3 Nguyen et al. (2009) predicting a loss rate of *ca.* 50 s^{-1} for CI-3 (via a VHP) and *ca.* 1 s^{-1} for
4 CI-4 (via ring closure to a dioxirane). This result is qualitatively consistent with the
5 experimental work of Ahrens et al. (2014), who determine a ratio of 85:15 for the abundance
6 of SCI-4:SCI-3 about 10 s after the initiation of the ozonolysis reaction, as a consequence of
7 the much faster decomposition rate of SCI-3. Thus the potential for bimolecular reactions to
8 compete with decomposition of SCI-3 and SCI-4 in the atmosphere is very different.
9 Nguyen et al. (2009) theoretically calculate a total SCI yield from β -pinene ozonolysis of 42
10 %, consisting of 16.2 % SCI-3, 20.6 % SCI-4, and 5.1 % CH_2OO . Ahrens et al. (2014) assume
11 an equal yield of CI-3 and CI-4 (45 %) with a 10 % yield of CH_2OO ; 40 % of the total C9-CI
12 are calculated to be stabilised at 1 atm. If all of the CH_2OO is assumed to be formed stabilised
13 (e.g. Nguyen et al., 2009) then this gives a total SCI yield of 46 %. Earlier experimental studies
14 have tended to determine lower total SCI yields with Hasson et al. (2001) reporting a total SCI
15 yield of 0.27 from measured product yields (almost entirely nopinone) and Hatakeyama et al.
16 (1984) reporting a total SCI yield of 0.25. Winterhalter et al. (2000) determined a yield of 0.16
17 (± 0.04) for excited CH_2OO from β -pinene ozonolysis, obtained via the nopinone yield and 0.35
18 for the stabilised C9-CI, giving a total SCI yield of 0.51 if all the CH_2OO is assumed to be
19 stabilised. Also, experimental studies have tended to report higher CH_2OO yields (determined
20 from measured nopinone yields) than theoretical studies. Nguyen et al. (2009) note that this
21 could be because nopinone can also be formed in bimolecular reactions of SCI-4, hence
22 experimental studies may overestimate CH_2OO production. The MCMv3.3.1 incorporates a
23 total SCI yield of 0.25 from β -pinene ozonolysis, with a yield of stabilised C9-CI of 0.102 and
24 a CH_2OO yield of 0.148.

25 1.2.3 Limonene derived SCI

26 Limonene has two double bonds at which ozone can react. Theory suggests that reaction at the
27 endocyclic bond is more likely; Baptista et al. (2011) calculate reaction at the endo-cyclic bond
28 to be 84 – 94 % (dependent on the level of theory applied). Zhang et al. (2006) suggest the
29 reaction at the endo-cyclic double bond to be roughly 25 times faster than at the exo-cyclic
30 bond, i.e. leading to a branching ratio of *ca.* 96 % reaction at the endo bond and the current
31 IUPAC recommendation (IUPAC, 2013) suggests about 95 % of the primary ozone reaction to
32 be at the endo bond. Leungsakul et al. (2005) reported a best fit to measurements from chamber

1 experiments by assuming an 85 % reaction at the endo-cyclic bond and 15 % at the exo-cyclic
2 bond.

3 Ozone reaction at the endo-cyclic bond of limonene produces four different C₁₀ CI (Scheme 4:
4 CI-5a, 5b, 6a, 6b). Similar to CI-1 and CI-2 from α -pinene, CI-5 is a mono-substituted CI for
5 which both *syn* (5a) and *anti* (5b) conformers exist, while the other, CI-6, is di-substituted, for
6 which two *syn*-conformers (6a and 6b) exist. Leungsakul et al. (2005) determined a total SCI
7 yield from limonene ozonolysis of 0.34, consisting of CH₂OO (0.05), CI-7 (0.04), CI-5 (0.15)
8 and CI-6 (0.11). Sipilä et al. (2014) determined a total SCI yield of 0.27 (\pm 0.12) from indirect
9 experiments measuring the production of H₂SO₄ from SO₂ oxidation in the presence of the
10 limonene-ozone system. The MCMv3.3.1 describes only reaction with ozone at the endocyclic
11 double bond and recommends a total SCI yield of 0.135 with stabilisation of only the mono-
12 substituted CI-5.

13

14 **2 Experimental**

15 **2.1 Experimental Approach**

16 The EUPHORE facility is a 200 m³ simulation chamber used primarily for studying reaction
17 mechanisms under atmospheric boundary layer conditions. Further details of the chamber setup
18 and instrumentation are available elsewhere (Becker, 1996; Alam et al., 2011), and a detailed
19 account of the experimental procedure, summarised below, is given in Newland et al (2015a).

20 Experiments comprised time-resolved measurement of the removal of SO₂ in the presence of
21 the monoterpene-ozone system, as a function of humidity. SO₂ and O₃ abundance were
22 measured using conventional fluorescence (reported precision \pm 1.0 ppbv) and UV absorption
23 monitors (reported precision \pm 4.5 ppbv), respectively; alkene abundance was determined via
24 FTIR spectroscopy. Experiments were performed in the dark (*i.e.* with the chamber housing
25 closed; $j(\text{NO}_2) \leq 10^{-6} \text{ s}^{-1}$), at atmospheric pressure (*ca.* 1000 mbar) and temperatures between
26 287 and 302 K. The chamber is fitted with large horizontal and vertical fans to ensure rapid
27 mixing (*ca.* 2 minutes). Chamber dilution was monitored via the first order decay of an aliquot
28 of SF₆, added prior to each experiment. Cyclohexane (*ca.* 75 ppmv) was added at the beginning
29 of each experiment to act as an OH scavenger, such that SO₂ reaction with OH was calculated
30 to be \leq 1 % of the total chemical SO₂ removal in all experiments.

Deleted: ,

1 Experimental procedure, starting with the chamber filled with clean scrubbed air, comprised
2 addition of SF₆ and cyclohexane, followed by water vapour, O₃ (ca. 500 ppbv) and SO₂ (ca. 50
3 ppbv). A gap of five minutes was left prior to addition of the monoterpene, to allow complete
4 mixing. The reaction was then initiated by addition of the monoterpene (ca. 400 ppbv for α-
5 pinene and β-pinene, ca. 200 ppbv for limonene), and reagent concentrations followed for
6 roughly 30 - 60 minutes; ca. 30 – 90 % of the monoterpene was consumed after this time,
7 dependent on the reaction rate with ozone. Four α-pinene + O₃, five β-pinene + O₃, and five
8 limonene + O₃ experiments, as a function of [H₂O], were performed in total. Each individual
9 run was performed at a constant humidity, with humidity varied to cover the range of [H₂O] =
10 0.1 – 19 × 10¹⁶ molecules cm⁻³, corresponding to an RH range of 0.1 – 28 % (at 298 K).
11 Measured increases in [SO₂] agreed with measured volumetric additions across the SO₂ and
12 humidity ranges used in the experiments (Newland et al., 2015a).

13 2.2 Analysis

14 A range of different SCI are produced from the ozonolysis of each of the three monoterpenes
15 (see Schemes 2–4), each with their own distinct chemical behaviour (*i.e.* yields, reaction rates);
16 it is therefore not feasible (from these experiments) to obtain data for each SCI independently;
17 consequently, for analytical purposes we necessarily treat the SCI population in a simplified
18 (lumped) manner – see Section 2.2.2.

19 SCI are assumed to be formed in the ozonolysis reaction with a yield ϕ (Reaction R1). They
20 can then react with SO₂, with H₂O, with acids formed in the ozonolysis reaction, with other
21 species present, or undergo unimolecular decomposition, under the experimental conditions
22 applied (Reactions R2 – R5). A fraction of the SCI produced reacts with SO₂. This fraction (f)
23 is the loss rate of the SCI to SO₂ ($k_2[\text{SO}_2]$) compared to the sum of the total loss processes for
24 the SCI (Equation E1) :

$$25 \quad f = \frac{k_2 [\text{SO}_2]}{k_2 [\text{SO}_2] + k_3 [\text{H}_2\text{O}] + k_a + k_s [\text{acid}] + L} \quad (\text{E1})$$

26 Here, L accounts for the sum of any other chemical loss processes for SCI in the chamber, with
27 the exception of reaction with acids these loss processes are expected to be negligible, as
28 discussed later. After correction for dilution, and neglecting other (non-alkene) chemical sinks
29 for O₃, such as reaction with HO₂ (also produced directly during alkene ozonolysis (Alam et

1 al., 2013; Malkin et al., 2010)), which was indicated through model calculations to account for
2 < 0.5 % of ozone loss under all the experimental conditions, the following equation is derived:

$$\frac{dSO_2}{dO_3} = \phi \cdot f \quad (E2)$$

3
4 From Equation E2, regression of the loss of ozone (dO_3) against the loss of SO_2 (dSO_2) for an
5 experiment at a given RH determines the product ϕ at a given point in time. This quantity will
6 vary through the experiment as SO_2 is consumed, and other potential SCI co-reactants are
7 produced, as predicted by Equation E1. A smoothed fit was applied to the experimental data
8 for the cumulative consumption of SO_2 and O_3 , ΔSO_2 and ΔO_3 , (as shown in Figure 2) to
9 determine dSO_2/dO_3 (and hence ϕ) at the start of each experiment, for use in Equation E2. The
10 start of each experiment (*i.e.* when $[SO_2] \sim 50$ ppbv) was used as this corresponds to the greatest
11 rate of production of the SCI, and hence largest experimental signals (*i.e.* greatest O_3 and SO_2
12 rate of change; greatest precision) and is the point at which the SCI + SO_2 reaction has the
13 greatest magnitude compared with any other potential loss processes for either reactant species
14 (see discussion below).

15 Other potential fates for SCIs include reaction with ozone (Kjaergaard et al., 2013; Vereecken
16 et al., 2014; Wei et al., 2014; Vereecken et al., 2015; Chang et al., 2018), with other SCI (Su
17 et al., 2014; Vereecken et al., 2014), carbonyl products (Taatjes et al., 2012), acids (Welz et al.,
18 2014), or with the parent alkene (Vereecken et al., 2014; Decker et al., 2017). Sensitivity
19 analyses using the most recent theoretical predictions (Vereecken et al., 2015) indicate that the
20 reaction with ozone is not significant under any of our experimental, accounting for less than
21 1.5% of SCI loss for *anti*-SCI (based on *anti*- CH_3CHO) at the lowest RH (worst case)
22 experiment. Generally, SCI loss to ozone is calculated to be < 1% for all SCI. Summed losses
23 from reaction with SCI (self-reaction), carbonyls and alkenes are likewise calculated to account
24 for < 1 % of the total SCI loss under the experimental conditions applied.

25 CH_2OO and CH_3CHO have been shown to react rapidly ($k = 1 - 5 \times 10^{-10} \text{ cm}^3 \text{ s}^{-1}$) with formic
26 and acetic acid (Welz et al., 2014). In ozonolysis experiments, Sipilä et al. (2014) determined
27 the relative reaction rate of acetic and formic acids with $(CH_3)_2COO$ (*i.e.* k_3/k_2) to be roughly
28 three. Organic acid mixing ratios in this work, as measured by FTIR, reached up to a few
29 hundreds of ppbv, suggesting these will likely be a significant SCI sink in our experiments. We
30 have therefore explicitly included reaction with organic acids in our analysis, incorporating the

Deleted: $f \cdot \phi$

Deleted: $f \cdot \phi$

Deleted: may be

Deleted: certain conditions

Deleted: up to 7

Deleted: However, generally

Deleted: 5

Deleted: *anti*-

Deleted: and < 1% for *syn*-SCI.

1 uncertainty arising from the (unknown) acid reaction rate constant, as described in Section
2 2.2.1.

3 The water dimer reactions of non-CH₂OO SCI are not considered in our analysis. The effect of
4 the water dimer reaction with C₁₀ and C₉ SCI (rather than the monomer) is expected to be minor
5 at the maximum [H₂O] (2 × 10¹⁷ cm⁻³) used in these experiments (< 30 % RH). Further, with
6 analogy to the *syn/anti*-CH₃CHOO system, for *syn*-SCI loss to the dimer (and monomer) will
7 not become competitive at the highest [H₂O] used here; for *anti*-SCI, the water monomer will
8 already be removing the majority of the SCI at the [H₂O] at which the dimer would become a
9 significant loss process, hence the dimer reaction is deemed unimportant. For CH₂OO, the
10 reaction rates with water and the water dimer have been quantified in recent EUPHORE
11 experimental studies, and the values from Newland et al. (2015a) are used in our analysis.

12 2.2.1 Derivation of $k(\text{SCI}+\text{H}_2\text{O})/k(\text{SCI}+\text{SO}_2)$ and $k_d/k(\text{SCI}+\text{SO}_2)$

13 As noted above, a range of different SCI are produced from the ozonolysis of the three
14 monoterpenes (see Schemes 2 – 4), each with their own distinct chemical behaviour, which
15 treated individually, introduce too many unknowns (*i.e.* yields, reaction rates) for explicit
16 analysis. Consequently for analytical purposes we treat the SCI population in a simplified
17 (lumped) manner:

18 Firstly, we use the simplest model possible, assuming that a single SCI is formed in each
19 ozonolysis reaction (Equation E3).

$$20 \quad \frac{f}{[\text{SO}_2]} = \left([\text{SO}_2] + \frac{k_3}{k_2} [\text{H}_2\text{O}] + \frac{k_d}{k_2} + \frac{k_5}{k_2} [\text{acid}] \right)^{-1} \quad (\text{E3})$$

21 In a second model, for each monoterpene, the SCI produced are assumed to belong to one of
22 two populations, denoted SCI-A and SCI-B. These two populations are split according to the
23 observation that the decomposition rates and reaction rates with water for the smaller SCI
24 (CH₃CHOO) have been predicted theoretically (Ryzhkov and Ariya, 2004; Kuwata et al., 2010;
25 Anglada et al., 2011) and shown experimentally (Taatjes et al., 2013; Sheps et al., 2014;
26 Newland et al., 2015a) to exhibit a strong dependence on the structure of the molecule. The
27 *syn*-CH₃CHOO conformer, which has the terminal oxygen of the carbonyl oxide moiety in the
28 *syn* position to the methyl group, has been shown to react very slowly with water and to readily
29 decompose, via the hydroperoxide mechanism; whereas the *anti*-CH₃CHOO conformer, with

Moved up [1]: To date, the effects of the water dimer, (H₂O)₂ on SCI removal have only been determined experimentally for CH₂OO (Berndt et al., 2014; Chao et al., 2015; Lewis et al., 2015; Newland et al., 2015a)

Deleted:). Theoretical calculations (Vereecken and Francisco, 2012) predicted the significant effect of the water dimer compared to the monomer for CH₂OO, but also that the ratio of the SCI + (H₂O)₂ : SCI + H₂O rate constants, k_d/k_3 , of the larger, more substituted SCI, *anti*-CH₃CHOO and (CH₃)₂COO, are 2 - 3 orders of magnitude smaller than for CH₂OO (Vereecken and Francisco, 2012). This would make the dimer reaction negligible at atmospherically accessible [H₂O] (*i.e.* < 1 × 10¹⁸ cm⁻³) for SCI larger than CH₂OO. Therefore, the effect of the water dimer reaction with C₁₀- and C₉-SCI is not considered in this analysis.

Formatted: Font color: Black

Formatted: Font color: Black

Formatted: Font:12 pt, Not Bold

Deleted: Secondly

1 the terminal oxygen of the carbonyl oxide moiety in the *anti*-position to the methyl group, has
 2 been shown to react fast with water and is not able to decompose via the hydroperoxide
 3 mechanism. Vereecken and Francisco (2012) have shown that all SCI studied theoretically with
 4 an alkyl group in the *syn* position have reaction rates with H₂O of $k < 4 \times 10^{-17}$ molecule cm³ s⁻¹
 5 (and for SCI larger than acetone oxide, $k < 8 \times 10^{-18}$ molecule cm³ s⁻¹).

6 We thus define two populations, assuming SCI-A (i.e. SCI that exhibit chemical properties of
 7 the *anti*-type SCI) to react fast with water and not to undergo unimolecular reactions, and SCI-
 8 B (i.e. SCI that exhibit chemical properties of the *syn* type SCI) to not react with water but to
 9 undergo unimolecular reactions. This simplification allows us to fit to the measurements using
 10 Equations E4 and E5, as shown below. The total SCI yields are determined by our experiments
 11 at high SO₂, and the relative yields of SCI-A and SCI-B are determined from fitting to Equation
 12 E5. These relative yields are then compared to those predicted from the literature.

13 In this model, $f = \gamma^A f^A + \gamma^B f^B$, where γ is the fraction of the total SCI yield (i.e. $\gamma^A + \gamma^B = 1$). f^A
 14 and f^B are the fractional losses of SCI-A and SCI-B to reaction with SO₂. Adapting Equation
 15 E1 to include the two SCI species gives Equation E4, where $k_5[acid]$ accounts for the SCI +
 16 acid reaction (see discussion of reaction rate constants below).

$$17 \quad f = \frac{\gamma^A k_2^A [SO_2]}{k_2^A [SO_2] + k_3 [H_2O] + k_5^A [acid]} + \frac{\gamma^B k_2^B [SO_2]}{k_2^B [SO_2] + k_d + k_5^B [acid]} \quad (E4)$$

18 Equation E4 can be rearranged to Equation E5 and fitted according to $f/[SO_2]$ derived from the
 19 measurements.

$$20 \quad \frac{f}{[SO_2]} = \frac{\gamma^A}{[SO_2] + \frac{k_3}{k_2^A} [H_2O] + \frac{k_5^A}{k_2^A} [acid]} + \frac{\gamma^B}{[SO_2] + \frac{k_d}{k_2^B} + \frac{k_5^B}{k_2^B} [acid]} \quad (E5)$$

21 Using values for γ^A and γ^B from the literature and varying the assumed values of the reaction of
 22 SCI with acid (k_5) allows us to determine k_3/k_2^A and k_d/k_2^B .

23 The assumptions made here allow analysis of a very complex system. However, a key
 24 consequence is that the relative rate constants obtained from the analysis presented here are not
 25 representative of the elementary reactions of any single specific SCI isomer formed, but rather
 26 represent a quantitative ensemble description of the integrated system, under atmospheric
 27 boundary layer conditions, which may be appropriate for atmospheric modelling. Additionally

1 our experimental approach cannot determine absolute rate constants (*i.e.* values of k_2 , k_3 , k_d) in
2 isolation, but is limited to assessing their relative values, measured under atmospheric
3 conditions, which may be placed on an absolute basis through use of an external reference value
4 (here the SCI + SO₂ rate constant).

5 2.2.2 SCI yield calculation

6 The value for the total SCI yield of each monoterpene, $\phi_{\text{SCI-TOT}}$, was determined from an
7 experiment performed under dry conditions (RH < 1%) in the presence of excess SO₂ (*ca.* 1000
8 ppbv), such that SO₂ scavenged the majority of the SCI. From Equation E2, regressing $d\text{SO}_2$
9 against $d\text{O}_3$ (corrected for chamber dilution), assuming f to be unity (*i.e.* all the SCI produced
10 reacts with SO₂), determines the value of ϕ_{min} , a lower limit to the SCI yield. Figure 1 shows
11 the experimental data, from which ϕ_{min} was derived.

12 In reality f will be less than one, at experimentally accessible SO₂ levels, as a fraction of the
13 SCI may still react with trace H₂O present, or undergo unimolecular reaction. The actual yield,
14 ϕ_{SCI} , was determined by combining the result from the excess-SO₂ experiment with those from
15 the series of experiments performed at lower SO₂, as a function of [H₂O], to obtain k_3/k_2 and
16 k_d/k_2 (see Section 2.2.1), through an iterative process to determine the single unique value of
17 ϕ_{SCI} which fits both datasets, as described in Newland et al. (2015a), but taking into account
18 the proposed model in this paper of there being two SCI produced. In this model, $f = \gamma^A f^A +$
19 $\gamma^B f^B$. Where $f^A = [\text{SO}_2] / ([\text{SO}_2] + k_3[\text{H}_2\text{O}]/k_2)$ and $f^B = [\text{SO}_2] / ([\text{SO}_2] + k_d/k_2)$ – other possible
20 SCI sinks are assumed to be negligible. In these excess-SO₂ experiments, $f^A \sim 1$ but $f^B < 1$ since
21 k_d still represents a significant sink.

22 γ^A (and hence γ^B , since $\gamma^B = 1 - \gamma^A$) is derived from fitting Equation E4 to the data from the
23 experiments performed at lower SO₂ for a given ϕ . Using a range of ϕ , gives a range of γ . These
24 different values of γ are used with the respective values of ϕ in fitting to Equation E4 to
25 determine values of k_3/k_2 and k_d/k_2 .

Formatted: Font:Italic, Subscript

26 [2.2.3 Experimental uncertainties](#)

27 [The uncertainty in \$k_3/k_2\$ was calculated by combining the mean relative errors from the precision](#)
28 [associated with the SO₂ and ozone measurements \(given in Section 2.1\) with the 2 \$\sigma\$ error and](#)
29 [the relative error in \$\phi\$, using the root of the sum of the squares of these four sources of error.](#)
30 [The uncertainty in \$k_d/k_2\$ was calculated in the same way.](#)

1 [The uncertainty in \$\phi_{\min}\$ was calculated by combining the uncertainty in \$\Delta SO_2\$ and \$\Delta O_3\$, as above.](#)
2 [The uncertainty in \$\phi\$ was calculated by applying the \$k_3/k_2\$ uncertainties and combining these](#)
3 [with the uncertainties in \$\phi_{\min}\$, using the root of the sum of the squares.](#)

5 3 Theoretical calculations

6 The rovibrational characteristics of all conformers of the CI formed from α -pinene and β -
7 pinene, the transition states for their unimolecular reaction, and for their reaction with H_2O ,
8 were characterized quantum chemically, first using the M06-2X/cc-pVDZ level of theory, and
9 subsequently refined at the M06-2X/aug-cc-pVTZ level. To obtain [the most](#) accurate barrier
10 heights for reaction, it has been shown (Berndt et al., 2015; Chhantyal-Pun et al., 2017; Fang
11 et al., 2016a, 2016b; Long et al., 2016; Nguyen et al., 2015) that post-CCSD(T) calculations
12 are necessary. [Performing](#) such calculations for the SCI discussed in this paper, with up to 14
13 non-hydrogen atoms, is well outside our computational resources. [Instead, we base our](#)
14 [predictions on high-level](#) CCSD(T)/aug-cc-pVTZ single point energy calculations, performed
15 for the reactions of nopinone oxides and the most relevant subset of pinonaldehyde oxides.
16 These data are [reliable](#) for relative rate estimates, but it remains useful to [further](#) improve the
17 absolute barrier height predictions, [as described](#) by Vereecken et al. (2017) [based on a data set](#)
18 [with](#) a large number of systematic calculations on smaller CI, allowing empirical corrections to
19 estimate the post-CCSD(T) barrier heights. [Briefly, they compare](#) rate coefficient calculations
20 against available harmonized experimental and very-high level theoretical kinetic rate
21 predictions, and adjusts the barrier heights by 0.4 to 2.6 kcal mol⁻¹ (depending on the base
22 methodology and the reaction type) to obtain best agreement with these benchmark results.

23 Using the energetic and rovibrational data thus obtained, multi-conformer transition state theory
24 (MC-TST) calculations (Truhlar et al., 1996; Vereecken and Peeters, 2003) were performed to
25 obtain the rate coefficient at 298K at the high pressure limit. All rate predictions incorporate
26 tunnelling corrections using an asymmetric Eckart barrier (Eckart, 1930; Johnston and
27 Heicklen, 1962). For the reaction of CI + H_2O , a pre-reactive complex is postulated at 7 kcal
28 mol⁻¹ below the free reactants, while the CI + $(H_2O)_2$ reaction is taken to have a pre-reactive
29 complex of 11 kcal mol⁻¹ stability. This pre-reactive complex affects tunnelling corrections; it
30 is assumed that this pre-reactive complex is always in equilibrium with the free reactants.

Formatted: Standard, Justified, Space Before: 6 pt, Line spacing: 1.5 lines

Deleted: Unfortunately, performing

Deleted: , though

Deleted: were

Deleted: unimolecular

Deleted: sufficient

Deleted: using the data set

Deleted: (Vereecken et al.,

Deleted:). This

Deleted: has

Deleted: the DFT or CCSD(T) barrier heights to

Deleted: The methodology for these corrections is described in more detail in Vereecken et al. (2017); briefly, it compares

1 In view of the high number of rotamers and the resulting computational cost, only a single
2 limonene-derived CI isomer was studied, where the TS for the CI + H₂O reaction was analyzed
3 at the M06-2X/cc-pVDZ level of theory with only a partial conformational analysis; a limited
4 number of the energetically most stable TS conformers thus discovered were re-optimized at
5 the M06-2X/aug-cc-pVTZ level of theory. These data will only be used for qualitative
6 assessments. However, we apply the structure-activity relationships (SARs) presented by
7 Vereecken et al. (Vereecken et al., 2017) to obtain an estimate of the rate coefficients, and
8 assess the role of the individual SCI isomers in limonene ozonolysis.

9 All quantum chemical calculations were performed using Gaussian-09 (Frisch et al., 2010).

10

11 **4 GEOS-Chem Model Simulation**

12 The global chemical transport model GEOS-Chem (v9-02, www.geos-chem.org, Bey et al.,
13 2002) is used to explore the spatial and temporal variability of the atmospheric impacts of the
14 experimentally derived chemistry. The model includes HO_x-NO_x-VOC-O₃-BrO_x chemistry
15 (Mao et al., 2010; Parrella et al., 2012) and a mass-based aerosol scheme. Biogenic
16 monoterpene emissions are taken from the Model of Emissions of Gases and Aerosols from
17 Nature (MEGAN) v2.1 inventory (Guenther et al., 2006; 2012). Transport is driven by
18 assimilated meteorology (GEOS-5) from NASA's Global Modelling and Assimilation Office
19 (GMAO). The model is run at 4°×5° resolution, with the second year (2005) used for analysis
20 and first year discarded as spin up.

21 In this study, the standard simulation was expanded to include emissions of seven monoterpene
22 species (α -pinene, β -pinene, limonene, myrcene, ocimene, carene, and sabinene) from MEGAN
23 v2.1. The ozonolysis scheme for each monoterpene, detailed in Section 7.1, considers the
24 formation of one or two types of SCI, and their subsequent reaction with SO₂, H₂O, or
25 unimolecular decomposition. [The reaction rates](#) of the monoterpenes with OH, O₃ and NO₃ [are](#)
26 detailed in Table S1.

27

Deleted: 6

Deleted: Reaction rate

Deleted: rare

1 5 Experimental Results

2 5.1 SCI Yield

3 Figure 1 shows the lower limit to the SCI yield, ϕ_{\min} , for the three monoterpenes, determined
4 from fitting Equation E5 to the experimental data. This gives values of 0.16 (± 0.01) for α -
5 pinene, 0.53 (± 0.01) for β -pinene and 0.20 (± 0.01) for limonene. These ϕ_{\min} values were then
6 corrected as described in Section 2.2.2 using the k_3/k_2 and k_d/k_2 values determined from the
7 measurements shown in Figures 3 – 5 using Equation E4. The corrected yields, ϕ_{SCI} , are 0.19
8 (± 0.01) for α -pinene, 0.60 (± 0.03) for β -pinene and 0.23 (± 0.01) for limonene. Uncertainties
9 are $\pm 2\sigma$, and represent the combined systematic (estimated measurement uncertainty) and
10 precision components. Literature yields for SCI production from monoterpene ozonolysis are
11 summarised in Table 1.

12 The value derived for the total SCI yield from α -pinene in this work of 0.19 agrees, within the
13 uncertainties, with the value of 0.15 (± 0.07) reported by Sipilä et al. (2014) and the value of
14 0.20 applied in the MCMv3.3.1.

15 The total SCI yield from β -pinene derived in this work, 0.60, agrees reasonably well with the
16 recent experimental work of Ahrens et al. (2014) who derived a total SCI yield of 0.50 (0.40
17 for the sum of CI-1 and CI-2 and 0.10 for CH_2OO , which is assumed to be formed almost
18 completely stabilised). The MCMv3.3.1 applies a total SCI yield of 0.25, of which 0.10 is a
19 C9-CI and 0.15 is CH_2OO . Earlier studies also tended to derive lower total SCI yields ranging
20 from 0.25 – 0.27 (Hasson et al., 2001; Hatakeyama et al., 1984).

21 The total SCI yield from limonene derived in this work, 0.23 (± 0.01) agrees with the recently
22 determined yield from Sipilä et al. (2014) of 0.27 (± 0.12). Leungsakul et al. (2005) derived a
23 somewhat higher yield of 0.34, while the MCMv3.3.1 applies a lower yield of 0.135.

24 5.2 $k_3(\text{SCI}+\text{H}_2\text{O})/k_2(\text{SCI}+\text{SO}_2)$ and $k_d/k_2(\text{SCI}+\text{SO}_2)$ Analysis

25 Figure 2 shows the loss of SO_2 as ozone is consumed by reaction with the monoterpene for each
26 of the three systems. Box modelling results suggest that $> 99\%$ of this SO_2 removal is caused
27 by reaction with SCI produced in the alkene-ozone reaction (rather than e.g. reaction with OH,
28 which is scavenged by cyclohexane). When the experiments are repeated at higher relative
29 humidity, the rate of loss of SO_2 decreases. This is as expected from Equation E1 and suggests

1 that there is competition between SO₂ and H₂O for reaction with the SCI produced, in
2 agreement with observations of smaller SCI, which demonstrate the same competition under
3 atmospherically relevant conditions (Newland et al., 2015a; Newland et al., 2015b).

4 However, as the relative humidity is increased further, the SO₂ loss does not fall to (near) zero
5 as would be expected from Equation E1. This suggests that at high [H₂O] the amount of SO₂
6 loss becomes less sensitive to [H₂O]. This is most likely due to there being at least two
7 chemically distinct SCI species present. This behaviour was previously observed for
8 CH₃CHOO by Newland et al. (2015a) and fits with the current understanding that the reactivity
9 of SCI is structure dependent.

10 To recap Section 2.2.1, the analysis presented here considers two models to fit the observations.
11 The first of these (Equation E3) assumes the formation of a single SCI species, which, in
12 addition to reacting with SO₂, can react with water, undergo unimolecular reaction or react with
13 acid. It is clearly evident from Figures 3 – 5 that this model does not give a good fit to the
14 observations for any of the monoterpene systems studied. Therefore, the results from this
15 (single SCI) approach are not discussed explicitly hereafter. The second of the models
16 (Equation E5) assumes the formation of two lumped, chemically distinct, populations of SCI,
17 denoted SCI-A and SCI-B. SCI-A is assumed to react fast with H₂O and to have minimal
18 decomposition. Conversely, SCI-B is assumed to have a negligible reaction with water under
19 the experimental conditions applied but to undergo rearrangement via a VHP. We use a least-
20 squares fit of Equation E5 to the data to determine the values of k_3/k_2 and k_d/k_2 . This approach
21 fits the data well (Figures 3 - 5) for all 3 monoterpenes and represents the overall attributes of
22 the SCI formed - but as noted, does not represent an explicit determination of individual
23 conformer-dependent rate constants.

24 5.2.1 α -pinene

25 The α -pinene system is sensitive to water vapour at the low H₂O range, with the SO₂ loss falling
26 dramatically when the RH is increased from 0.1 to 2.5 % (Figure 2). However, at higher RH
27 the SO₂ loss appears to be rather insensitive to [H₂O].

28 CI-1 can be formed in either a *syn* (1a) or *anti* (1b) configuration, whereas both CI-2 conformers
29 formed are in a *syn* configuration (see Scheme 2). For one of the two conformers of CI-2 (CI-
30 2b), the hydrogen atom available for abstraction by the terminal oxygen of the carbonyl oxide
31 group is attached to the carbon on the four-membered ring. This has been shown in the β -pinene

1 system to make a large difference with respect to the ability of the hydrogen to be abstracted
2 and to undergo the VHP mechanism (Rickard et al., 1999; Nguyen et al., 2009). This therefore
3 suggests that CI-2b may exhibit characteristics of both SCI-A and SCI-B. Ma et al. (2008) infer
4 a probable equal yield of the two basic CI structures. This would suggest a relative yield for
5 SCI-A of 0.25 – 0.50 (depending on the precise nature of CI-2b). Fitting Equation E4 to the
6 data and allowing lambda to vary determines values of $\gamma^A = 0.40$ and $\gamma^B = 0.60$ (Figure 3).

7 In Figure 3, Equation E4 is fitted to the α -pinene measurements, assuming
8 $k(\text{SCI+acid})/k(\text{SCI+SO}_2) = 0$. This derives a minimum value for $k(\text{SCI-A+H}_2\text{O})/k(\text{SCI-}$
9 $\text{A+SO}_2)$, the water dependent fraction of the SCI, and a maximum value for
10 $k(\text{decomposition:SCI-B})/k(\text{SCI-B+SO}_2)$, the water independent fraction of the SCI. The kinetic
11 parameters derived from the fitting are displayed in Table 2.

12 Figure 6 shows the variation of the derived k_3/k_2 and k_d/k_2 values as the ratio k_5/k_2 ,
13 $k(\text{SCI+acid})/k(\text{SCI+SO}_2)$, is varied from zero to one. The derived k_3/k_2 increases by about 40
14 % from $1.4 (\pm 0.34) \times 10^{-3}$ to $2.0 (\pm 0.49) \times 10^{-3}$. The derived k_d/k_2 value decreases, again by
15 about 40 %, from $8.2 (\pm 1.5) \times 10^{12} \text{ cm}^{-3}$ to $5.1 (\pm 0.93) \times 10^{12} \text{ cm}^{-3}$.

16 The derived limits to the relative rate constants can be put on an absolute scale using the
17 $k(\text{SCI+SO}_2)$ values for CH_3CHOO from Sheps et al. (2014) for the *syn* and *anti* conformers.
18 These are, *syn*: $2.9 \times 10^{-11} \text{ cm}^3 \text{ s}^{-1}$ and *anti*: $2.2 \times 10^{-10} \text{ cm}^3 \text{ s}^{-1}$. The *syn* rate constant is applied
19 to the derived $k(\text{decomposition:SCI-B})/k(\text{SCI-B+SO}_2)$ value and the *anti* rate constant to the
20 $k(\text{SCI-A+H}_2\text{O})/k(\text{SCI-A+SO}_2)$ value. It should be noted that the k_2 values are for quite different
21 SCI to those formed in this study and to our knowledge no structure specific $k(\text{SCI+SO}_2)$ have
22 been reported for monoterpene derived SCI, though Ahrens et al. (2014) determine an average
23 $k_2 \sim 4 \times 10^{-11} \text{ cm}^3 \text{ s}^{-1}$ for SCI derived from β -pinene, i.e. a value within an order of magnitude
24 of those determined for the smaller SCI CH_2OO , CH_3CHOO and $(\text{CH}_3)_2\text{COO}$ (e.g. Welz et al.,
25 2012; Taatjes et al., 2013; Sheps et al., 2014; Huang et al., 2015). Using the Sheps et al. (2014)
26 values yields $k(\text{SCI-A+H}_2\text{O}) > 3.1 (\pm 0.75) \times 10^{-13} \text{ cm}^3 \text{ s}^{-1}$ and $k(\text{decomposition:SCI-B}) < 240$
27 $(\pm 44) \text{ s}^{-1}$ (using the values derived for $k(\text{SCI-A+acid})/k(\text{SCI-A+SO}_2) = 0$). This k_3 value is an
28 order of magnitude larger than the rate constants determined for the smaller *anti*- CH_3CHOO in
29 the direct studies of Sheps et al. (2014) ($2.4 \times 10^{-14} \text{ cm}^3 \text{ s}^{-1}$) and Taatjes et al. (2013) ($1.0 \times 10^{-}$
30 $14 \text{ cm}^3 \text{ s}^{-1}$). The decomposition value derived for SCI-B is of the same order of magnitude as
31 that for *syn*- CH_3CHOO ($348 \pm 332 \text{ s}^{-1}$) and $(\text{CH}_3)_2\text{COO}$ ($819 \pm 190 \text{ s}^{-1}$) from Newland et al.,
32 (2015a) (using updated direct measurement values of k_2 from Sheps et al. (2014) and Huang et

1 al. (2015) for *syn*-CH₃CHOO and (CH₃)₂COO respectively) and within the range from the
2 recent paper by Smith et al. (2016) which derives a decomposition rate for (CH₃)₂COO of 269
3 (± 82) s⁻¹ at 283 K increasing to 916 (± 56) s⁻¹ at 323 K.

4 Sipilä et al. (2014) applied a single-SCI analysis approach to the formation of H₂SO₄ from SO₂
5 oxidation in the presence of the α -pinene ozonolysis system. They determined that for α -pinene,
6 $k_d \gg k(\text{SCI}+\text{H}_2\text{O})[\text{H}_2\text{O}]$ for $[\text{H}_2\text{O}] < 2.9 \times 10^{17} \text{ cm}^{-3}$, i.e. that the fate of SCI formed in the
7 system is rather insensitive to $[\text{H}_2\text{O}]$. Across the $[\text{SO}_2]$ and RH ranges used in their study, the
8 results obtained here would indicate H₂O to always be the dominant sink for SCI-A, i.e. the fact
9 that Sipilä et al. (2014) see similar H₂SO₄ production across the RH range in their study is
10 consistent with these results.

11

12 5.2.2 β -pinene

13 Two recent studies (Nguyen et al., 2009; Ahrens et al., 2014) have suggested yields of the two
14 C₉-CI (CI-3 and CI-4, see Scheme 3) obtained from β -pinene ozonolysis to be roughly equal.
15 In these studies Ahrens et al. (2014) assume a CH₂OO yield of 0.10 while Nguyen et al. (2009)
16 determine theoretically the yield of CH₂OO to be 0.05. Another theoretical study (Zhang and
17 Zhang, 2005) predicted a CH₂OO yield of 0.08. In experimental studies, Winterhalter et al.
18 (2000) determined the CH₂OO yield to be 0.16 (± 0.04) from measuring the nopinone yield and
19 assuming it to be entirely a primary ozonolysis product (i.e. the co-product of CH₂OO
20 formation) and Ma and Marston (2008) determine a summed contribution of 84 % (± 0.03) for
21 the two C₉-CI (i.e. a 16 % CH₂OO yield). The theoretical studies are somewhat lower than the
22 experimental but Nguyen et al. (2009) note that CI-4 is likely to form additional nopinone in
23 bimolecular reactions. The CH₂OO is assumed to all be formed stabilised (e.g. Nguyen et al.
24 2009).

25 SCI-3 is expected to undergo unimolecular reactions at least an order of magnitude faster than
26 SCI-4 (Nguyen et al., 2009; Ahrens et al., 2014). The reaction of SCI-3 with water is expected
27 to be slow based on the calculations presented in Table 4, with a pseudo first order reaction rate
28 of 0.3 s^{-1} at the highest $[\text{H}_2\text{O}]$ used here, $2 \times 10^{17} \text{ cm}^{-3}$, 298 K, whereas the water reaction with
29 SCI-4 is expected to be considerably faster with a pseudo first order reaction rate of 85 s^{-1} at
30 $[\text{H}_2\text{O}] = 2 \times 10^{17} \text{ cm}^{-3}$, 298 K. This reaction would thus be expected to be competitive with
31 reaction with SO₂ for SCI-4 under the experimental conditions employed. This is in agreement

Deleted: 1.

Deleted: 75 % RH

Deleted: 240

Deleted: 75 % RH

Deleted: will

Deleted: likely

Deleted: the dominant fate of

Deleted: at typical atmospheric RH.

Deleted: that

1 with the observations of Ma and Marston (2008), which show a clear dependence of nopinone
2 formation on RH (presumed to be formed from SCI + H₂O). Fitting Equation E4 to the data
3 determines values of $\gamma^A = 0.41$ and $\gamma^B = 0.59$ (Figure 4).

4 Using these values, and assuming $k(\text{SCI+acid})/k(\text{SCI+SO}_2) = 0$, yields a $k(\text{SCI-A+H}_2\text{O})/k(\text{SCI-}$
5 $\text{A+SO}_2)$ value of $> 1.0 (\pm 0.27) \times 10^{-4}$ and a $k(\text{decomposition:SCI-B})/k(\text{SCI-B+SO}_2)$ value of $<$
6 $6.0 (\pm 1.3) \times 10^{12} \text{ cm}^{-3}$ (Table 2).

7 As shown in Figure 6, increasing k_3/k_2 , $k(\text{SCI+acid})/k(\text{SCI+SO}_2)$, from zero to one, decreases
8 the derived k_d/k_2 from $6.0 (\pm 1.3) \times 10^{12} \text{ cm}^{-3}$ to $1.8 (\pm 0.39) \times 10^{12} \text{ cm}^{-3}$. The derived k_3/k_2
9 increases by a factor of four from $1.0 (\pm 0.27) \times 10^{-4}$ to $3.7 (\pm 1.0) \times 10^{-4}$.

10 These values can be put on an absolute scale (using the values derived above for $k_3/k_2 = 0$). For
11 SCI-A, $k(\text{SCI+SO}_2)$ is taken as the experimentally determined value of $4 \times 10^{11} \text{ cm}^3 \text{ s}^{-1}$ from
12 Ahrens et al. (2014). For SCI-B, the *syn*-CH₃CHOO $k(\text{SCI+SO}_2)$ value determined by Sheps et
13 al. (2014) is used. This gives values of $k(\text{SCI-A+H}_2\text{O}) > 4 \times 10^{-15} (\pm 1) \text{ cm}^3 \text{ s}^{-1}$ and
14 $k(\text{decomposition:SCI-B}) < 170 (\pm 38) \text{ s}^{-1}$.

15 5.2.3 Limonene

16 For the limonene measurements presented in Figure 2, $(d\text{SO}_2/d\text{O}_3)/dt$ appears to be non-linear,
17 with a jump in $d\text{SO}_2/d\text{O}_3$ between 120 and 150 ppbv of ozone consumed. This is most evident
18 in the two lowest RH runs (0.2 and 2.0 %). Limonene is the fastest reacting of the systems
19 presented here, with the alkene reaction having consumed 100 ppbv of ozone within the first
20 five minutes. The limonene sample required about five minutes of heating before the entire
21 sample was volatilized and injected into the chamber. This therefore may account for the
22 apparent non-linear nature of $d\text{SO}_2/d\text{O}_3$ in Figure 2.

23 The SO₂ loss in the limonene-ozone system is less affected by increasing H₂O than for either α
24 or β -pinene (Figure 5), with the values of $f/[\text{SO}_2]$ (y-axis) varying by roughly a factor of two
25 over the RH range applied compared to more than a factor of three variation for the other two
26 systems. Hence it might be expected that there is little formation of H₂O dependent SCI or that
27 it has a rather slow reaction rate with water.

28 Fitting Equation E4 to the data determines values of $\gamma^A = 0.22$ and $\gamma^B = 0.78$ (Figure 5). This is
29 broadly in line with the ratio recommended in the MCMv3.3.1 of 0.27:0.73, and with that
30 proposed in Leungsakul et al. (2005) who use a CI-A:CI-B ratio of 0.35:0.65, but also include
31 some stabilisation of CH₂OO and C₉-CI from ozone reaction at the exo-cyclic bond. This yields

1 a $k(\text{SCI-A}+\text{H}_2\text{O})/k(\text{SCI-A}+\text{SO}_2)$ value of $< 3.5 (\pm 0.20) \times 10^{-5}$ and a $k(\text{decomposition:SCI-}$
2 $\text{B})/k(\text{SCI-B}+\text{SO}_2)$ value of $> 4.5 (\pm 0.10) \times 10^{12} \text{ cm}^{-3}$.

3 Figure 6 shows that the derived k_d/k_2 increases by about 7 % as $k(\text{SCI+acid})/k(\text{SCI}+\text{SO}_2)$ ranges
4 from 0.0 to 0.8. The derived k_3/k_2 becomes negative at $k(\text{SCI+acid})/k(\text{SCI}+\text{SO}_2) > 0.8$, putting
5 an upper limit on this ratio, i.e. $k_3/k_2 < 0.8$, for the limonene system.

6 Putting these values on an absolute scale (using the values derived for $k_3/k_2 = 0$), using the
7 CH_3CHOO *syn* and *anti* $k(\text{SCI}+\text{SO}_2)$ determined by Sheps et al. (2014), yields values of < 7.7
8 $(\pm 0.60) \times 10^{-15} \text{ cm}^3 \text{ s}^{-1}$ and $> 130 (\pm 3) \text{ s}^{-1}$ for k_3 and k_d respectively. These values are similar
9 to those derived for the SCI-A and SCI-B formed from β -pinene. The k_3 value is a factor of
10 three smaller than that determined by Sheps et al. (2014) for $k_3(\text{anti-CH}_3\text{CHOO}+\text{H}_2\text{O})$, $2.4 \times$
11 $10^{-14} \text{ cm}^3 \text{ s}^{-1}$.

12 Sipilä et al. (2014) applied a single-SCI analysis approach to the formation of H_2SO_4 from SO_2
13 oxidation by the limonene ozonolysis system and determined that, similarly to α -pinene,
14 $k(\text{decomp.}) \gg k(\text{SCI}+\text{H}_2\text{O})[\text{H}_2\text{O}]$ for $[\text{H}_2\text{O}] < 2.9 \times 10^{17} \text{ cm}^{-3}$, i.e. that the system is rather
15 insensitive to $[\text{H}_2\text{O}]$. Our data are consistent with the limonene system being less sensitive to
16 $[\text{H}_2\text{O}]$ than the SCI populations derived from the other two monoterpenes reported here.

17 5.2.4 Experimental Summary

18 The reaction rates of SCI-A (i.e. SCI that exhibit chemical properties of the *anti*-type SCI)
19 derived from the three different monoterpenes with water range from < 0.8 to $> 31 \times 10^{-14} \text{ cm}^3$
20 s^{-1} , broadly in line with the derived rates of Sheps et al. (2014) for *anti-CH}_3\text{CHOO} of $2.4 \times 10^{-}$
21 $14 \text{ cm}^3 \text{ s}^{-1}$. The decomposition rates of SCI-B (i.e. SCI that exhibit chemical properties of the
22 *syn*-type SCI) are on the order of 100 - 250 s^{-1} . This is in line with those derived for *syn*-
23 CH_3CHOO from *cis* and *trans*-but-2-ene ozonolysis and $(\text{CH}_3)_2\text{COO}$ by Newland et al. (2015a)
24 of 348 (± 332) s^{-1} and 819 (± 190) s^{-1} respectively (assuming $k(\text{syn-CH}_3\text{CHOO}+\text{SO}_2) = 2.9 \times$
25 $10^{-11} \text{ cm}^3 \text{ s}^{-1}$ (Sheps et al., 2014) and $k((\text{CH}_3)_2\text{COO}+\text{SO}_2) = 2.9 \times 10^{-10} \text{ cm}^3 \text{ s}^{-1}$ (Huang et al.,
26 2015)) and recent results from Smith et al. (2016) of 269 – 916 s^{-1} (strongly dependent on
27 temperature) for $(\text{CH}_3)_2\text{COO}$ decomposition. In this work we only derive relative rates, but the
28 similarity of the k_3 and k_d values derived when the k_2 values for *syn* and *anti-CH}_3\text{CHOO} from
29 Sheps et al. (2014) are applied is consistent with the recent work of Ahrens et al. (2014),
30 suggesting that large SCI, derived from monoterpenes, demonstrate a similar reactivity towards
31 SO_2 as smaller SCI. One uncertainty in the derivation of the kinetics presented herein is the**

Deleted: The removal of SO_2 in the presence of ozonolysis reactions of α -pinene, β -pinene and limonene has been studied as a function of water vapour concentration, and analysed following the approximation that the SCI population can be represented through a two species model, with contrasting unimolecular decomposition rates and reactivity to water. The results presented in this work suggest that all three monoterpenes studied produce a range of SCI that have differing reactivities towards water and decomposition. This is in agreement with current theoretical understanding but is the first experimental demonstration for large SCI derived from monoterpene ozonolysis. The complex reactivity of the systems investigated is further highlighted by the fact that the experimental data are not fitted well by the assumption of the formation of a single SCI species. While the behaviour of large SCI derived from monoterpenes are likely to be significantly more complicated than is accounted for by simply considering the differing kinetics of *syn* and *anti* SCI conformers, this approach provides a reasonable description of the experimental behaviour observed, and the results presented here are broadly in line with experimental results from the smaller SCI and from theoretical results.

1 reactions of the SCI produced with organic acids. These acids were present in the experiments
2 (owing to formation in the monoterpene ozonolysis reactions themselves) at levels which may
3 have been a competitive sink for the SCI.

4 **6 Theoretical results and comparison to experiments**

5 The theoretically predicted rate coefficients for unimolecular reactions of the monoterpene SCI
6 are listed in Table 3, while those for the reaction with H₂O are listed in Table 4. These data can
7 be compared against the experimental data obtained in this work.
8

9 **6.1.1 α -pinene**

10 The theory-based rate coefficients show one pinonaldehyde oxide, CI-1b, with a rate of reaction
11 with water that is significantly faster than the remaining α -pinene-derived CI. Comparing this
12 rate to the experimental data suggests that CI-1b corresponds to SCI-A, with matching rate
13 coefficients within an order of magnitude, i.e. within the expected uncertainty. We thus deduce
14 that SCI-A is CI-1b. The remaining pinonaldehyde oxides, CI-1a, CI-2a and CI-2b, react
15 predominantly through unimolecular reactions, where theory-based rate coefficients range from
16 60 to 600 s⁻¹, all within a factor of 4 of the experimentally derived population-averaged rate of
17 240 ± 44 s⁻¹, i.e. matching within the uncertainty margins. The unimolecular rate coefficients
18 of this set of CI are sufficiently close that it is not feasible to separate these in the experimental
19 data, so we can only conclude that SCI-B in the α -pinene ozonolysis experiments may consist
20 of a mixture of C-1a, CI-2a and CI-2b.

21 **6.1.2 β -pinene**

22 The theoretical analysis for nopinone oxides shows one isomer, SCI-4, that has a fast rate of
23 reaction with water, but a slow unimolecular isomerisation, while the other isomer, SCI-3,
24 shows a fast unimolecular decomposition. These can thus be unequivocally equated to the
25 experimentally obtained SCI-A and SCI-B, respectively, inasmuch as the yield of CH₂OO is
26 minor. The predicted rate coefficients are within the expected uncertainty intervals of the
27 theoretical data, a factor of 5 for the unimolecular rates, and an order of magnitude for the
28 reaction with H₂O.

29 The experimental rate measurements are defined relative to the reaction rate with SO₂; the value
30 adopted for the $k(\text{SCI}+\text{SO}_2)$ reaction therefore influences the derived rate coefficient values.

Deleted: The ability of the simplified SCI-A / SCI-B approach to fit the experimental data and the good agreement with theory and experimental work for smaller SCI suggests that the kinetic parameters derived herein, using a lumped two-SCI system, may be useful for modelling and provide the best available basis for modelling the effects of SCI on atmospheric SO₂ oxidation in the presence of water vapour. To this end, in Section 6 we present the results of a global modelling study using the kinetic parameters derived herein.

Formatted: Heading 1

1 Ahrens et al. (2014) directly measured the SO₂ rate coefficient of the longest-lived SCI (SCI-
2 4) to be $\sim 4 \times 10^{-11} \text{ cm}^3 \text{ s}^{-1}$, but for SCI-3 we assume a similar rate coefficient as *syn*-CH₃CHOO
3 + SO₂ determined by Sheps et al. (2014) of $2.9 \times 10^{-11} \text{ cm}^3 \text{ s}^{-1}$. Nopinone oxides are bicyclic
4 compounds, with a bulky dimethyl-substituted 4-membered ring adjacent to the carbonyl oxide
5 moiety. To examine the potential impact of steric hindrance on the SCI + SO₂ reaction, we
6 characterized all sulfur-substituted secondary ozonides (S-SOZ) formed in this reaction
7 (Kuwata et al., 2015; Vereecken et al., 2012). We find that the tri-cyclic S-SOZ shows very
8 little interaction between the sulfur-bearing ring and the β-pinene substituents, and little change
9 in ring strain. The energies of the S-SOZ adducts relative to the SCI + SO₂ reactants thus
10 remains very similar to that of CH₂OO, CH₃CHOO or (CH₃)₂COO, confirming the quality of
11 our selection of reference rate coefficients.

12 6.1.3 Limonene

13 Of the six non-CH₂OO CI formed in limonene ozonolysis, CI-5b was predicted to have a fast
14 reaction rate with H₂O; its oxide substitution patterns is similar to pinonaldehyde oxide CI-1b.
15 The SAR-predicted rate coefficient of CI-5b + H₂O is within a factor of 2 of the experimentally
16 derived k_3 value for SCI-A, such that we can equate SCI-A to CI-5b with confidence. The SCI-
17 B set of Criegee intermediates then contains the summed population of the remaining five CI,
18 all of which react slowly with H₂O. The SAR-predicted unimolecular decay rate coefficients
19 range from 15 to 700 s⁻¹, all within a factor of 9 of the experimentally obtained $k_d = 130 \text{ s}^{-1}$; it
20 should be noted that for limonene-derived CI, no explicit theoretical calculations are available,
21 and the SAR-predictions carry a somewhat larger uncertainty.
22 We have performed an exhaustive characterisation of the conformers of CI-5b. The most stable
23 conformers show an internal complex formation between the oxide moiety and the carbonyl
24 group, similar to those characterized for the bimolecular reaction of CI with carbonyl
25 compounds (Jalan et al., 2013; Wei et al., 2015). The theoretical study by Jiang et al. (2013) on
26 limonene ozonolysis appears to have omitted internal rotation and cannot be compared directly.
27 It seems likely that the limonene-derived CI can thus easily undergo internal SOZ formation,
28 which is thought (Vereecken and Francisco, 2012) to be entropically unfavourable, but to have
29 a low barrier to reaction. For α-pinene, a similar internal complex formation and SOZ ring
30 closure is not as favourable due to the geometric limitations enforced by the 4-membered ring.
31 A large number of transition state conformers for CI-5b + H₂O were characterized, though no
32 exhaustive search was completed. The energetically most favourable structures show

1 interaction between the carbonyl group, and the H₂O co-reactant as it adds onto the carbonyl
2 oxide moiety. Similar stabilising interactions between the carbonyl moiety and the
3 carbonyl oxide moiety were reported recently in cyclohexene-derived CI
4 (Berndt et al., 2017). This interaction thus lowers the barrier to reaction though it is currently
5 unclear whether it enhances the reaction rate compared to e.g. the α -pinene-derived CI-1b, as
6 these hydrogen-bonded structures are entropically not very favourable. The intra-molecular
7 interactions with heterosubstituents could be investigated in future work.

8

9 **7 Global modelling study**

10 **7.1 SCI Chemistry**

11 A global atmospheric modelling study was performed using the GEOS-Chem chemical
12 transport model (as described in Section 4) to examine the global monoterpene derived SCI
13 budget and the contribution of these SCI to gas-phase SO₂ oxidation. The existing chemistry
14 scheme in the model is supplemented with monoterpene SCI chemistry based on the
15 experimental results described in Section 5 and in Table 5. It should be noted here that this
16 modelling study focuses on the chemical impacts of monoterpene SCI formed from ozonolysis
17 reactions only. No chemistry for other SCIs derived from isoprene and/or other (smaller)
18 alkenes are incorporated in the adapted model chemical scheme used.

19 The monoterpene emissions in GEOS-Chem are taken from MEGAN v2.1 (Guenther et al.,
20 2012). The scheme emits seven monoterpenes: α -pinene, β -pinene, limonene, myrcene,
21 ocimene, 3-carene, and sabinene. The monoterpenes are oxidised within the model by OH, NO₃
22 and O₃ at rates shown in Table S1. Reaction with O₃ leads to the production of monoterpene
23 specific SCI. Reactions with OH and NO₃ does not lead to the formation of any products, with
24 the reactions only acting as a sink for the monoterpene and the respective oxidant. The SCI
25 yields from the ozonolysis of α -pinene, β -pinene, and limonene are derived from the
26 experimental work presented here. SCI from each monoterpene are split in to SCI-A and SCI-
27 B as defined in previous sections. For the other four monoterpenes emitted, the SCI yields, and
28 kinetics are derived based on similarity of structure to one of the species studied here or
29 previously in the literature. The main SCI produced in the ozonolysis of myrcene and ocimene
30 are expected to be acetone oxide ((CH₃)₂COO) or 4-vinyl-5-hexenal oxide
31 (CH₂CHC(CH₂)CH₂CH₂CHOO), since ozone has been suggested to react predominantly at the

1 internal double bond (~97 % for myrcene, ~90% for ocimene (Baker et al., 2004)). The SCI
2 yield is taken to be 0.30, similar to that of (CH₃)₂COO from 2,3-dimethyl-but-2-ene ozonolysis
3 (Newland et al., 2015a). However, this may be an underestimate since it has been predicted that
4 stabilisation of small CI increases with an increasing size of carbonyl co-product, as this co-
5 product can take more of the nascent energy of the primary ozonide on decomposition due to a
6 greater number of degrees of freedom available (Nguyen et al., 2009, Newland et al., 2015b).
7 Sabinene is a bicyclic monoterpene with an external double bond and hence is treated like β-
8 pinene. This assumption is backed up by recent theoretical work (Wang and Wang, 2017), who
9 predict similar behaviour of sabinene derived SCI to the predicted behaviour of β-pinene SCI
10 by Nguyen et al. (2009a). They predict a SCI yield between 24 % - 64 %. 3-carene is a bicyclic
11 monoterpene with an internal double bond and is treated like α-pinene.

Deleted: isolated

12 7.2 Modelling Results

13 Figure 7 shows the annually averaged total SCI burden from monoterpene ozonolysis in the
14 surface layer in the GEOS-Chem simulation. A number of interesting features are apparent
15 from this figure and the associated information given in Table 6:

- 16 (i) The highest annually averaged monoterpene SCI concentrations are found above
17 tropical forests.
- 18 (ii) Peak annually averaged monoterpene SCI concentrations are $\sim 1.4 \times 10^4 \text{ cm}^{-3}$.
- 19 (iii) > 97 % of the total monoterpene SCI burden is SCI-B.

Deleted: 2

20 Annual global monoterpene emissions are dominated by the tropics (Figure S1), accounting for
21 > 90 % during the northern hemisphere winter months (November – April) and 70 % even
22 during the peak emissions from the northern boreal region during June and July (Sindelarova
23 et al., 2014). Despite annually averaged surface ozone mixing ratios being roughly a factor of
24 2 higher in the northern mid-high latitudes, monoterpene SCI production is still dominated by
25 the tropics. Annually averaged surface monoterpene SCI concentrations across the northern
26 boreal regions are $< 2 \times 10^3 \text{ cm}^{-3}$; during the summer months (JJA) this value rises to $2 - 5 \times$
27 10^3 cm^{-3} .

28 More than 97 % of the total monoterpene derived SCI are SCI-B (Table 6). This is because
29 typical water vapour concentrations in the tropics are $> 5.0 \times 10^{17} \text{ cm}^{-3}$. This gives SCI-A
30 removal rates (i.e. $k_3[\text{H}_2\text{O}]$) of $2 \times 10^3 - 1.5 \times 10^5 \text{ s}^{-1}$, whereas removal rates of SCI-B to
31 unimolecular reactions have been determined here to be 1 – 3 orders of magnitude slower, on

1 the order of 100 - 250 s⁻¹. Since the loss of SCI-B is independent of temperature in the model,
2 the highest SCI-B concentrations would be expected to be located in the regions of highest SCI-
3 B production. Recent experimental studies (Smith et al., 2016) have demonstrated a strong
4 temperature dependence for the unimolecular decomposition rate of (CH₃)₂COO between 283
5 and 323 K (269 – 916 s⁻¹). Therefore, it may be that in reality there would be some geographical
6 variation in the rate of unimolecular loss.

7 The monoterpene SCI-A + H₂O reactions are expected to lead to high yields of both large (e.g.
8 Ma et al., 2008; Ma and Marston, 2008) and small (measured in high yield in the experiments
9 presented here) organic acids.

10 Figure 8 shows the seasonal removal of SO₂ by reaction with monoterpene derived SCI, as a
11 percentage of total gas-phase SO₂ oxidation in the surface layer. Monoterpene SCI are most
12 important (relative to OH) for SO₂ oxidation over tropical forests, where they account for up to
13 60 % of the local gas-phase SO₂ removal during DJF and MAM in some regions. The reasons
14 for this are two-fold: firstly, the highest modelled monoterpene SCI concentrations are found
15 in these regions (Figure 7); but additionally, OH concentrations in the model are low over these
16 areas (Figure S2). Historically there has been discrepancies between modelled and observed
17 OH concentrations over tropical forests, with models appearing to under-predict [OH] by up to
18 a factor of ten (e.g. Lelieveld et al., 2008). It was proposed that this was due to missing sources
19 of OH recycling during isoprene oxidation. During recent years there have been advances in
20 our understanding of isoprene chemistry. GEOS-Chem v-09, used here, includes an isoprene
21 OH recycling scheme largely based on Paulot et al. (2009a, 2009b), with updates from Peeters
22 et al. (2009), Peeters and Müller (2010), and Crouse et al. (2011; 2012), and evaluated in Mao
23 et al. (2013). However, more recent experimental and theoretical work is not yet included.

24 Annually, monoterpene SCI oxidation accounts for 1.2 % of the gas-phase SO₂ oxidation in the
25 terrestrial tropics. This accounts for the removal of 2.9 Gg of SO₂. Across the northern boreal
26 forests, monoterpene SCI contribute 0.7 % to gas-phase SO₂ removal annually, removing 0.8
27 Gg of SO₂. Globally, throughout the whole atmosphere, monoterpene SCI account for only 0.5
28 % of gas-phase SO₂ removal, removing 8.1 Gg of SO₂ annually.

29 It is noted that MEGAN does not contain oceanic monoterpene emissions, which may increase
30 the global importance of SCI for gas-phase SO₂ removal. Luo and Yu (2010) determined annual
31 global oceanic α-pinene emissions to be 29.5 TgC using a top-down approach, with only 0.013
32 (Luo and Yu, 2010) – 0.26 (Hackenberg et al., 2017) TgC estimated using a range of bottom-

Deleted: 50

Deleted: 1

Deleted: 5

Deleted: 5

Deleted: 6

Deleted: 4

Deleted: 6.

1 up approaches; clearly there are large uncertainties in oceanic monoterpene emissions. At the
2 upper end of this range they could potentially provide a similar contribution to SCI production
3 and subsequent SO₂ oxidation as monoterpenes emitted from the terrestrial biosphere. SCI
4 production more generally could be further amplified by sources such as marine-derived alkyl
5 iodine photolysis.

6 Blitz et al. (2017) recently calculated a revised SO₂ + OH reaction rate (k_I (1 bar N₂) (298 K) =
7 $5.8 \times 10^{-13} \text{ cm}^3 \text{ s}^{-1}$), based on experimental work and a master equation analysis, which is ~ 40
8 % lower than the rate given in the most recent JPL data evaluation (Burkholder et al., 2015)
9 (k_I (1 bar N₂) (298 K) = $9.5 \times 10^{-13} \text{ cm}^3 \text{ s}^{-1}$), which is used in the GEOS-Chem model
10 simulation. Figure S3 shows the increased influence of monoterpene derived SCI on gas-phase
11 SO₂ oxidation if the alternative SO₂ + OH rate is used. This increased the impact of
12 monoterpene SCI to up to 67 % of gas-phase SO₂ removal in regions of the tropical forests
13 during DJF and MAM, with the contribution of monoterpene SCI to global gas-phase SO₂
14 oxidation increasing to 0.7 %.

15 While certain monoterpenes appear to be more important than others with regard to the
16 production of SCI which will oxidise SO₂, these results are sensitive to the kinetics used and
17 the assumptions made for the monoterpenes not studied experimentally here. Hence we do not
18 attempt to draw any conclusions about the relative importance of each monoterpene from the
19 modelling. Clearly the most important monoterpenes will be those with high yields of SCI-B,
20 particularly if those SCI-B have a structure that hinders unimolecular decomposition (such as
21 certain β -pinene derived SCI).

22 ▲ 23 8 Conclusions

24 We report results from an integrated experimental (simulation chamber), theoretical (quantum
25 chemical) and modelling (global chemistry-transport simulation) study of the impacts of
26 monoterpene ozonolysis reactions on stabilised Criegee intermediate (SCI) formation and SO₂
27 oxidation. The ozonolysis of the monoterpenes α -pinene, β -pinene and limonene have been
28 shown to produce a structurally diverse range of chemically distinct SCIs, with some showing
29 limited sensitivity to / reaction with water vapour under near-atmospheric humidity levels. A
30 multi-component system is required to explain the experimentally observed SO₂ removal
31 kinetics. A two-body model system based on the assumption of a fraction of the SCI produced
32 being reactive towards water (SCI-A; potentially contributing to the significant formation of a

Deleted: 60

Deleted: 6

Formatted: Font:9 pt

Formatted: Standard, Justified

Deleted: <#>Discussion and Atmospheric Implica... [1]

1 range of organic acids in the atmosphere), and a fraction being relatively unreactive towards
2 water (SCI-B), analogous to the structural dependencies observed for the simpler CH₃CHO
3 SCI system, has been shown to describe the observed kinetic data reasonably well for all the
4 monoterpene systems investigated, and may form a computationally affordable and
5 conceptually accessible basis for the description of this chemistry within atmospheric models.

6 Moreover such an approach is required to accurately predict SCI concentrations, which will be
7 underestimated if a simple average of the properties of the two different SCI classes is used.

8 The atmospheric fate of SCI-B produced from the monoterpenes studied here will be controlled
9 by their removal by unimolecular decomposition. In this work, we have experimentally
10 determined the monoterpene SCI-B decomposition rate to be between 100 and 250 s⁻¹. This has
11 significant implications for the role of monoterpene derived SCI as oxidants in the atmosphere.
12 The fate of SCI-A will be reaction with water or the water dimer, likely leading to the
13 production of a range of organic acids.

14 A theory-based analysis of the kinetics of the SCI formed from α-pinene, β-pinene ozonolysis
15 has also been performed, which complements the experimental work. The identification of the
16 likely SCI-A and SCI-B populations and the derived kinetics agree with experimental
17 observations within the respective uncertainties.

18 A modelling study using the GEOS-Chem global 3-D chemical transport model supplemented
19 with the chemical kinetics elucidated in this work suggests that the global monoterpene derived
20 SCI burden will be dominated (> 97%) by SCI-B. The highest annually averaged SCI
21 concentrations are found in the tropics, with seasonally averaged monoterpene SCI
22 concentrations up to $1.4 \times 10^4 \text{ cm}^{-3}$ owing to large monoterpene emissions. Across the boreal
23 forest, average SCI concentrations reach between $3 - 5 \times 10^3 \text{ cm}^{-3}$ during the northern
24 hemisphere summer. Oxidation of SO₂ by monoterpene SCI is shown to also be most important
25 in the tropics. While oxidation by SCI contributes < 1% to gas-phase SO₂ oxidation globally,
26 over tropical forests this can rise to up to 60 % at certain times of the year. Monoterpene SCI
27 driven SO₂ oxidation will increase the production of sulfate aerosol –affecting atmospheric
28 radiation transfer, and hence climate; and reduce the atmospheric lifetime and hence transport
29 of SO₂. These effects will be substantial in areas where monoterpene emissions are significant,
30 in particular over the Amazon, Central Africa and SE Asian rainforests.

31

32 Data Availability

Deleted: 2

Deleted: 50

Deleted: -

1 Experimental data will be made available in the Eurochamp database (www.eurochamp.org)
2 from the H2020 EUROCHAMP2020 project, GA n°730997

3

4 **Acknowledgements**

5 The assistance of the EUPHORE staff is gratefully acknowledged., Salim Alam, Marie
6 Camredon and Stephanie La are thanked for helpful discussions. This work was funded by EU
7 FP7 EUROCHAMP 2 Transnational Access activity (E2-2012-05-28-0077) and the UK NERC
8 Projects (NE/K005448/1, Reactions of Stabilised Criegee Intermediates in the Atmosphere:
9 Implications for Tropospheric Composition & Climate) and (NE/M013448/1, Mechanisms for
10 Atmospheric chemistry: GenerationN, Interpretation and Fidelity - MAGNIFY). Fundación
11 CEAM is partly supported by Generalitat Valenciana, and the project DESESTRES (Prometeo
12 Program - Generalitat Valenciana). EUPHORE instrumentation is partly funded by the Spanish
13 Ministry of Science and Innovation, through INNPLANTA project: PCT-440000-2010-003.
14 LV is indebted to the Max Planck Graduate Center with the Johannes Gutenberg-Universität
15 Mainz (MPGC).

16

1 **References**

- 2 Ahrens, J., Carlsson, P. T. M., Hertl, N., Olzmann, M., Pfeifle, M., Wolf, J. L., and Zeuch, T.:
3 Infrared Detection of Criegee Intermediates Formed during the Ozonolysis of β -pinene and
4 Their Reactivity towards Sulfur Dioxide, *Angew. Chem. Int. Ed. Engl.*, **53**, 715–719, 2014.
- 5 Alam, M. S., Camredon, M., Rickard, A. R., Carr, T., Wyche, K. P., Hornsby, K. E., Monks,
6 P. S., and Bloss, W. J.: Total radical yields from tropospheric ethene ozonolysis, *Phys. Chem.*
7 *Chem. Phys.*, **13**, 11002–11015, 2011.
- 8 Alam, M. S., Rickard, A. R., Camredon, M., Wyche, K. P., Carr, T., Hornsby, K. E., Monks,
9 P. S., and Bloss, W. J.: Radical Product Yields from the Ozonolysis of Short Chain Alkenes
10 under Atmospheric Boundary Layer Conditions, *J. Phys. Chem. A*, **117**, 12468-12483, 2013.
- 11 Anglada, J. M., Gonzalez, J., and Torrent-Sucarrat, M.: Effects of the substituents on the
12 reactivity of carbonyl oxides. A theoretical study on the reaction of substituted carbonyl oxides
13 with water, *Phys. Chem. Chem. Phys.*, **13**, 13034–13045, 2011.
- 14 Anglada, M. and Sole, A.: Impact of the water dimer on the atmospheric reactivity of carbonyl
15 oxides, *Phys. Chem. Chem. Phys.*, **18**, 17698-17712, 2016.
- 16 Asatryan, R. and Bozzelli, J.W.: Formation of a Criegee intermediate in the low-temperature
17 oxidation of dimethyl sulfoxide, *Phys. Chem. Chem. Phys.*, **10**, 1769–1780, 2008.
- 18 Baptista, L., Pfeifer, L., da Silva, E. C., and Arbilla, G.: Kinetics and Thermodynamics of
19 Limonene Ozonolysis, *J. Phys. Chem. A*, **115**, 10911-10919, 2011.
- 20 Beck, M., Winterhalter, R., Herrmann, F., and Moortgat, G. K.: The gas-phase ozonolysis of α -
21 humulene, *Phys. Chem. Chem. Phys.*, **13**, 10970–11001, 2011.
- 22 Becker, K. H.: EUPHORE: Final Report to the European Commission, Contract EV5V-CT92-
23 0059, Bergische Universität Wuppertal, Germany, 1996.
- 24 Berndt, T., Voigtländer, J., Stratmann, F., Junninen, H., Mauldin III, R. L., Sipilä, M., Kulmala,
25 M., and Herrmann, H.: Competing atmospheric reactions of CH_2OO with SO_2 and water
26 vapour, *Phys. Chem. Chem. Phys.*, **16**, 19130–19136, 2014.
- 27 Berndt, T., Kaethner, R., Voigtländer, J., Stratmann, F., Pfeifle, M., Reichle, P., Sipilä, M.,
28 Kulmala, M., and Olzmann, M.: Kinetics of the unimolecular reaction of CH_2OO and the
29 bimolecular reactions with the water monomer, acetaldehyde and acetone at atmospheric
30 conditions, *Phys. Chem. Chem. Phys.*, **17**, 19862–19873, 2015.

1 Berndt, T., Herrmann, H. and Kurtén, T.: Direct probing of Criegee intermediates from gas-
2 phase ozonolysis using chemical ionization mass spectrometry, *J. Am. Chem. Soc.*, DOI:
3 10.1021/jacs.7b05849, 2017.

4 Berresheim, H., Adam, M., Monahan, C., O'Dowd, C., Plane, J. M. C., Bohn, B., and Rohrer
5 F.: Missing SO₂ oxidant in the coastal atmosphere? – observations from high-resolution
6 measurements of OH and atmospheric sulfur compounds, *Atmos. Chem. Phys.*, 14, 12209-
7 12223, 2014.

8 Bey, I., Jacob, D. J., Yantosca, R. M., Logan, J. A., Field, B. D., Fiore, A. M., Li, Q., Liu, H.
9 Y., Mickley, L. J., and Schultz, M. G.: Global modelling of tropospheric chemistry with
10 assimilated meteorology: Model description and evaluation, *J. Geophys. Res.*, 106, 23073–
11 23095, 2001.

12 Blitz, M. A., Salter, R. J., Heard, D. E., and Seakins, P. J.: An Experimental and Master
13 Equation Study of the Kinetics of OH/OD + SO₂: The Limiting High-Pressure Rate
14 Coefficients, *J. Phys. Chem. A*, 121, 3184-3191, 2017.

15 [Burkholder, J. B., Sander, S. P., Abbatt, J., Barker, J. R., Huie, R. E., Kolb, C. E., Kurylo, M.](#)
16 [J., Orkin, V. L., Wilmouth, D. M., and Wine, P. H.:](#) Chemical Kinetics and Photochemical Data
17 for Use in Atmospheric Studies, Evaluation No. 18, JPL Publication 15-10, Jet Propulsion
18 Laboratory, Pasadena, 2015 <http://jpldataeval.jpl.nasa.gov>.

19 Caravan, R. L., Khan, A. H. M., Rotavera, B., Papajak, E., Antonov, I. O., Chen, M. -W., Au,
20 K., Chao, W., Osborn, D. L., Lin, J. J. -M., Percival, C. J., Shallcross, D. E., and Taatjes, C. E.:
21 Products of Criegee intermediate reactions with NO₂: experimental measurements and
22 tropospheric implications, *Faraday Discuss.*, 200, 313-330, 2017.

23 [Chang, Y.-P., Chang, H.-H. and Lin, J. J.-M.:](#) Kinetics of the simplest Criegee intermediate
24 [reaction with ozone studied using a mid-infrared quantum cascade laser spectrometer,](#) *Phys.*
25 [Chem. Chem. Phys., 20, 97–102, doi:10.1039/c7cp06653h, 2018.](#)

26 Chao, W., Hsieh, J. -T., Chang, C. -H., and Lin, J. J. -M.: Direct kinetic measurement of the
27 reaction of the simplest Criegee intermediate with water vapour, *Science*, DOI:
28 10.1126/science.1261549, 2015.

29 Chen, L., Wang, W., Wang, W., Liu, Y., Liu, F., Liu, N., and Wang, B.: Water-catalyzed
30 decomposition of the simplest Criegee intermediate CH₂OO, *Theor. Chem. Acc.*, 135:131, DOI
31 10.1007/s00214-016-1894-9, 2016.

Deleted: J. B.

Deleted: S. P.

Deleted: J.

Deleted: . R.

Deleted: . E.

Deleted: C

Deleted: .

Deleted: M. J.

Deleted: V. L.

Deleted: D. M.

Deleted: P. H.

Deleted: "

Deleted: ,"

1 Chhantyal-Pun, R., Davey, A., Shallcross, D. E., Percival, C. J., and Orr-Ewing, A. J.: A kinetic
2 study of the CH₂OO Criegee intermediate self-reaction, reaction with SO₂ and
3 unimolecular reaction using cavity ring-down spectroscopy, *Phys. Chem. Chem. Phys.*, 17,
4 3617-3626, 2015.

5 Chhantyal-Pun, R., Welz, O., Savee, J. D., Eskola, A. J., Lee, E. P. F., Blacker, L., Hill, H. R.,
6 Ashcroft, M., Khan, M. A. H. H., Lloyd-Jones, G. C., Evans, L. A., Rotavera, B., Huang, H.,
7 Osborn, D. L., Mok, D. K. W., Dyke, J. M., Shallcross, D. E., Percival, C. J., Orr-Ewing, A. J.
8 and Taatjes, C. A.: Direct Measurements of Unimolecular and Bimolecular Reaction Kinetics
9 of the Criegee Intermediate (CH₃)₂COO, *J. Phys. Chem. A*, 121, 4-15, 2017

10 Chuong, B., Zhang, J. and Donahue, N. M.: Cycloalkene Ozonolysis: Collisionally Mediated
11 Mechanistic Branching, *J. Am. Chem. Soc.*, 126, 12363-12373, 2004.

12 Cox, R. A., and Penkett, S. A.: Oxidation of atmospheric SO₂ by products of the ozone-olefin
13 reaction, *Nature*, 230, 321-322, 1971.

14 Crouse, J. D., Paulot, F., Kjaergaard, H. G., and Wennberg, P. O.: Peroxy radical isomerization
15 in the oxidation of isoprene, *Phys. Chem. Chem. Phys.*, 13, 13607-13613, 2011.

16 Crouse, J. D., Knap, H. C., Ørnsø, K. B., Jørgensen, S., Paulot, F., Kjaergaard, H. G., and
17 Wennberg, P. O.: Atmospheric fate of methacrolein. 1. Peroxy radical isomerization following
18 addition of OH and O₂, *J. Phys. Chem. A*, 116, 5756-5762, 2012.

19 Decker, Z. C. J., Au, K., Vereecken, L., and Sheps, L.: Direct experimental probing and
20 theoretical analysis of the reaction between the simplest Criegee intermediate and CH₂OO and
21 isoprene, *Phys. Chem. Chem. Phys.*, 19, 8541-8551, 2017.

22 Donahue, N. M., Drozd, G. T., Epstein, S. A., Presto, A. A., and Kroll, J. H.: Adventures in
23 ozoneland: down the rabbit-hole, *Phys. Chem. Chem. Phys.*, 13, 10848-10857, 2011.

24 Drozd, G. T., and Donahue, N. M.: Pressure Dependence of Stabilized Criegee Intermediate
25 Formation from a Sequence of Alkenes, *J. Phys. Chem. A*, 115, 4381-4387, 2011.

26 Eckart, C.: The penetration of a potential barrier by electrons, *Phys. Rev.*, 35, 1303-1309, 1930.

27 Ehn, M., Thornton, J. A., Kleist, E., Sipilä, M., Junninen, H., Pulli- nen, I., Springer, M.,
28 Rubach, F., Tillmann, R., Lee, B., Lopez- Hilfiker, F., Andres, S., Acir, I.-H., Rissanen, M.,
29 Jokinen, T., Schobesberger, S., Kangasluoma, J., Kontkanen, J., Nieminen, T., Kurtén, T.,
30 Nielsen, L. B., Jørgensen, S., Kjaergaard, H. G., Canagaratna, M., Maso, M. D., Berndt, T.,

1 Petäjä, T., Wahner, A., Kerminen, V.-M., Kulmala, M., Worsnop, D. R., Wildt, J., and Mentel,
2 T. F.: A large source of low-volatility secondary organic aerosol., *Nature*, 506, 476–479,
3 doi:10.1038/nature13032, 2014.

4 Fang, Y., Liu, F., Barber, V. P., Klippenstein, S. J., McCoy, A. B. and Lester, M. I.:
5 Communication: Real time observation of unimolecular decay of Criegee intermediates to OH
6 radical products, *J. Chem. Phys.*, 144, 2016a.

7 Fang, Y., Liu, F., Klippenstein, S. J. and Lester, M. I.: Direct observation of unimolecular decay
8 of CH₃CH₂CHOO Criegee intermediates to OH radical products, *J. Chem. Phys.*, 145, 2016b.

9 Fenske, J. D., Hasson, A. S., Ho, A. W., and Paulson, S. E.: Measurement of absolute
10 unimolecular and bimolecular rate constants for CH₃CHOO generated by the trans-2-butene
11 reaction with ozone in the gas phase, *J. Phys. Chem. A*, 104, 9921–9932, 2000.

12 Foreman, E. S., Kapnas, K. M., and Murray, C.: Reactions between Criegee Intermediates and
13 the Inorganic Acids HCl and HNO₃: Kinetics and Atmospheric Implications, *Angew. Chem.*
14 *Int. Ed.*, 55, 1–5, 2016.

15 Frisch, M. J., Trucks, G. W., Schlegel, H. B., Scuseria, G. E., Robb, M. A., Cheeseman, J. R.,
16 Scalmani, G., Barone, V., Mennucci, B., Petersson, G. A., Nakatsuji, H., Caricato, M., Li, X.,
17 Hratchian, H. P., Izmaylov, A. F., Bloino, J., Zheng, G., Sonnenberg, J. L., Hada, M., Ehara,
18 M., Toyota, K., Fukuda, R., Hasegawa, J., Ishida, M., Nakajima, T., Honda, Y., Kitao, O.,
19 Nakai, H., Vreven, T., Montgomery Jr., J. A., Peralta, J. E., Ogliaro, F., Bearpark, M., Heyd, J.
20 J., Brothers, E., Kudin, K. N., Staroverov, V. N., Keith, T., Kobayashi, R., Normand, J.,
21 Normand, J., Raghavachari, K., Rendell, A., Burant, J. C., Iyengar, S. S., Tomasi, J., Cossi, M.,
22 Rega, N., Millam, J. M., Klene, M., Knox, J. E., Cross, J. B., Bakken, V., Adamo, C., Jaramillo,
23 J., Gomperts, R., Stratmann, R. E., Yazyev, O., Austin, A. J., Cammi, R., Pomelli, C.,
24 Ochterski, J. W., Martin, R. L., Morokuma, K., Zakrzewski, V. G., Voth, G. A., Salvador, P.,
25 Dannenberg, J. J., Dapprich, S., Daniels, A. D., Farkas, O., Foresman, J. B., Ortiz, J. V.,
26 Cioslowski, J., Fox, D. J. and Pople, J. A.: *Gaussian 09*, Revision B.01, Gaussian Inc.,
27 Wallington CT., 2010.

28 Gravestock, T. J., Blitz, M. A., Bloss, W. J., and Heard, D. E.: A multidimensional study of the
29 reaction CH₂I+O₂: Products and atmospheric implications, *ChemPhysChem*, 11, 3928 – 3941,
30 2010.

1 Guenther, A., Karl, T., Harley, P., Wiedinmyer, C., Palmer, P. I., and Geron, C.: Estimates of
2 global terrestrial isoprene emissions using MEGAN (Model of Emissions of Gases and
3 Aerosols from Nature), *Atmos. Chem. Phys.*, 6, 3181-3210, 2006.

4 Guenther, A. B., Jiang, X., Heald, C. L., Sakulyanontvittaya, T., Duhl, T., Emmons, L. K., and
5 Wang, X.: The Model of Emissions of Gases and Aerosols from Nature version 2.1
6 (MEGAN2.1): an extended and updated framework for modeling biogenic emissions, *Geosci.*
7 *Model Dev.*, 5, 1471-1492, 2012.

8 Gutbrod, R., Schindler, R. N., Kraka, E., and Cremer, D.: Formation of OH radicals in the gas
9 phase ozonolysis of alkenes: the unexpected role of carbonyl oxides, *Chem. Phys. Lett.*, 252,
10 221–229, 1996.

11 Hackenberg S. C., Andrews, S. J., Airs, R. L., Arnold, S. R., Bouman, H. A., Cummings, D.,
12 Lewis, A. C., Minaeian, J. K., Reifel, K. M., Small, A., Tarran, G. A., Tilstone, G. H., and
13 Carpenter, L. J.: Basin-Scale Observations of Monoterpenes in the Arctic and Atlantic Oceans,
14 *Environ. Sci. Technol.*, 51, 10449–10458, 2017.

15 Hasson, A. S., Ho, A. W., Kuwata, K. T., and Paulson, S. E.: Production of stabilized Criegee
16 intermediates and peroxides in the gas phase ozonolysis of alkenes 2. Asymmetric and biogenic
17 alkenes, *J. Geophys. Res.*, 106, 34143–34153, 2001.

18 Hatakeyama, S., Kobayashi, H., and Akimoto, H.: Gas-Phase Oxidation of SO₂ in the Ozone-
19 Olefin Reactions, *J. Phys. Chem.*, 88, 4736-4739, 1984.

20 Huang, H. -L., Chao, W., and Lin, J. J. -M.: Kinetics of a Criegee intermediate that would
21 survive at high humidity and may oxidize atmospheric SO₂, *Proc. Natl. Acad. Sci.*, 112, 10857–
22 10862, 2015.

23 IUPAC Task Group on Atmospheric Chemical Kinetic Data Evaluation – Data Sheet
24 Ox_VOC20, (<http://iupac.pole-ether.fr>), 2013.

25 [IUPAC Task Group on Atmospheric Chemical Kinetic Data Evaluation – Data Sheet](#)
26 [CGI_14 \(CH₃\)₂COO + M, \(<http://iupac.pole-ether.fr>\), 2017.](#)

27 Jalan, A., Allen, J. W., and Green, W. H.: Chemically activated formation of organic acids in
28 reactions of the Criegee intermediate with aldehydes and ketones, *Phys. Chem. Chem. Phys.*,
29 15, 16841-16852, 2013.

Formatted: Font:LiberationSerif, 12 pt

1 Jenkin, M. E., Saunders, S. M., and Pilling, M. J.: The tropospheric degradation of volatile
2 organic compounds: a protocol for mechanism development, *Atmos. Environ.*, 31, 81–104,
3 1997.

4 Jenkin, M. E., Young, J. C., and Rickard, A. R.: The MCM v3.3.1 degradation scheme for
5 isoprene, *Atmos. Chem. Phys.*, 15, 11433-11459, 2015.

6 Jiang, L., Lan, R., Xu, Y. -S., Zhang, W. -J., Yang, W.: Reaction of stabilized criegee
7 intermediates from ozonolysis of limonene with water: Ab initio and DFT study, *Int. J. Mol.*
8 *Sci.*, 14, 5784-5805, 2013.

9 Johnson, D. and Marston, G.: The gas-phase ozonolysis of unsaturated volatile organic
10 compounds in the troposphere, *Chem. Soc. Rev.*, 37, 699–716, 2008.

11 Johnston, H. S. and Heicklen, J.: Tunneling corrections for unsymmetrical Eckart potential
12 energy barriers, *J. Phys. Chem.*, 66, 532–533, 1962.

13 Kidwell, N. M., Li, H., Wang, X., Bowman, J. M., and Lester, M. I.: Unimolecular dissociation
14 dynamics of vibrationally activated CH₃CHOO Criegee intermediates to OH radical products,
15 *Nature Chemistry*, 8, 509-514, 2016.

16 Kirkby, J., et al.: Ion-induced nucleation of pure biogenic particles, *Nature*, 533, 521-526, 2016.

17 Kjaergaard, H. G., Kurtén, T., Nielsen, L. B., Jørgensen, S., and Wennberg, P. O.: Criegee
18 Intermediates React with Ozone, *J. Phys. Chem. Lett.*, 4, 2525-2529, 2013.

19 Kotzias, D., Fytianos, K., and Geiss, F.: Reactions of monoterpenes with ozone, sulphur dioxide
20 and nitrogen dioxide – Gas phase oxidation of SO₂ and formation of sulphuric acid, *Atmos.*
21 *Environ.*, 24, 2127-2132, 1990.

22 Kroll, J., Donahue, N. M., Cee, V. J., Demerjian, K. L., and Anderson, J. G.: Gas-phase
23 ozonolysis of alkenes: formation of OH from anti carbonyl oxides, *J. Am. Chem. Soc.*, 124,
24 8518–8519, 2002.

25 Kuwata, K. T., Guinn, E., Hermes, M. R., Fernandez, J., Mathison, J. and Huang, K.: A
26 Computational Re-Examination of the Criegee Intermediate-Sulfur Dioxide Reaction, *J. Phys.*
27 *Chem. A*, 119, 10316-10335, 2015.

28 Kuwata, K. T., Hermes, M. R., Carlson, M. J., and Zogg, C. K.: Computational Studies of the
29 Isomerization and Hydration Reactions of Acetaldehyde Oxide and Methyl Vinyl Carbonyl
30 Oxide, *J. Phys Chem. A*, 114, 9192-9204, 2010.

- 1 Lelieveld, J., Butler, T. M., Crowley, J. N., Dillon, T. J., Fischer, H., Ganzeveld, L., Harder,
2 H., Lawrence, M. G., Martinez, M., Taraborrelli, D., and Williams, J.: Atmospheric oxidation
3 capacity sustained by a tropical forest, *Nature*, 452, 737-740, 2008.
- 4 Leungsakul, S., Jaoui, M., and Kamens, R. M.: Kinetic Mechanism for Predicting Secondary
5 Organic Aerosol Formation from the Reaction of *d*-limonene with Ozone, *Environ. Sci.*
6 *Technol.*, 39, 9583-9594, 2005.
- 7 Lewis, T. R., Blitz, M. A., Heard, D. E., and Seakins, P. W.: Direct evidence for a substantive
8 reaction between the Criegee intermediate, CH₂OO, and the water vapour dimer, *Phys. Chem.*
9 *Chem. Phys.*, 17, 4859-4863, 2015.
- 10 Lin, L., Chang, H., Chang, C., Chao, W., Smith, M. C., Chang, C., Lin, J. J., and Takahashi,
11 K.: Competition between H₂O and (H₂O)₂ reactions with CH₂OO/CH₃CHOO, *Phys. Chem.*
12 *Chem. Phys.*, 18, 4557-4568, 2016a.
- 13 [Lin, L., -C., Chao, W., Chang, C. -H., Takahashi, K., and Lin, J. J. -M.: Temperature dependence
14 of the reaction of: Anti-CH₃CHOO with water vapor, *Phys. Chem. Chem. Phys.*, 18, 28189-
15 28197, 2016b.](#)
- 16 [Liu, Y., Liu, F., Liu, S., Dai, D., Dong, W., and Yang, X.: A kinetic study of the CH₂OO Criegee
17 intermediate reaction with SO₂, \(H₂O\)₂, CH₂I₂ and I atoms using OH laser induced
18 fluorescence, *Phys. Chem. Chem. Phys.*, 19, 20786-20794, 2017.](#)
- 19 Long, B., Bao, J. L. and Truhlar, D. G.: Atmospheric Chemistry of Criegee Intermediates.
20 Unimolecular Reactions and Reactions with Water, *J. Am. Chem. Soc.*, 138, 14409-14422,
21 2016.
- 22 Luo, G., and Yu, F.: A numerical evaluation of global oceanic emissions of α -pinene and
23 isoprene, *Atmos. Chem. Phys.*, 10, 2007-2015, 2010.
- 24 Ma, Y., Russell, A. T., and Marston, G.: Mechanisms for the formation of secondary organic
25 aerosol components from the gas-phase ozonolysis of α -pinene, *Phys. Chem. Chem. Phys.*, 10,
26 4294-4312, 2008.
- 27 Ma, Y., and Marston, G.: Multi-functional acid formation from the gas-phase ozonolysis of β -
28 pinene, *Phys. Chem. Chem. Phys.*, 10, 6115-6126, 2008.
- 29 Mao, J., Jacob, D. J., Evans, M. J., Olson, J. R., Ren, X., Brune, W. H., St. Clair, J. M., Crouse,
30 J. D., Spencer, Beaver, M. R., Wennberg, P. O., Cubison, M. J., Jimenez, J. L., Fried, A.,

Deleted: 2016

1 Weibring, P., Walega, J. G., Hall, S. R., Weinheimer, A. J., Cohen, R. C., Chen, G., Crawford,
2 J. H., Jaeglé, L., Fisher, J. A., Yantosca, R. M., Le Sager, P., and Carouge, C.: Chemistry of
3 hydrogen oxide radicals (HOx) in the Arctic troposphere in spring, *Atmos. Chem. Phys.*, 10,
4 5823-5838, 2010.

5 Mao, J., Paulot, F., Jacob, D. J., Cohen, R. C., Crouse, J. D., Wennberg, P. O., Keller, C. A.,
6 Hudman, R. C., Barkley, M. P., and Horowitz, L. W.: Ozone and organic nitrates over the
7 eastern United States: Sensitivity to isoprene chemistry, *J. Geophys. Res.*, 118, 11256–11268,
8 2013.

9 Martinez, R. I., and Herron, J. T.: Stopped-flow studies of the mechanisms of alkene-ozone
10 reactions in the gas-phase: tetramethylethylene, *J. Phys. Chem.*, 91, 946-953, 1987.

11 Mauldin III, R. L., Berndt, T., Sipilä, M., Paasonen, P., Petäjä, T., Kim, S., Kurtén, T.,
12 Stratmann, F., Kerminen, V.-M., and Kulmala, M.: A new atmospherically relevant oxidant,
13 *Nature*, 488, 193–196, 2012.

14 Newland, M. J., Rickard, A. R., Alam, M. S., Vereecken, L., Muñoz, A., Ródenas, M., and
15 Bloss, W. J.: Kinetics of stabilised Criegee intermediates derived from alkene ozonolysis:
16 reactions with SO₂, H₂O and decomposition under boundary layer conditions, *Phys. Chem.*
17 *Chem. Phys.*, 17, 4076, 2015a.

18 Newland, M. J., Rickard, A. R., Vereecken, L., Muñoz, A., Ródenas, M., and Bloss, W. J.:
19 Atmospheric isoprene ozonolysis: impacts of stabilised Criegee intermediate reactions with
20 SO₂, H₂O and dimethyl sulfide, *Atmos. Chem. Phys.*, 15, 9521–9536, 2015b.

21 Nguyen, T. L., Peeters, J., and Vereecken, L.: Theoretical study of the gas-phase ozonolysis of
22 β-pinene (C₁₀H₁₆), *Phys. Chem. Chem. Phys.*, 11, 5643–5656, 2009a.

23 Nguyen, T. L., Winterhalter, R., Moortgat, G., Kanawati, B., Peeters, J., and Vereecken, L.:
24 The gas-phase ozonolysis of β-caryophyllene (C₁₅H₂₄). Part II: A theoretical study, *Phys. Chem.*
25 *Chem. Phys.*, 11, 4173–4183, 2009b.

26 Nguyen, T. L., Lee, H., Matthews, D. A., McCarthy, M. C. and Stanton, J. F.: Stabilization of
27 the Simplest Criegee Intermediate from the Reaction between Ozone and Ethylene: A High
28 Level Quantum Chemical and Kinetic Analysis of Ozonolysis, *J. Phys. Chem. A*, 119, 5524-
29 5533, 2015.

1 Niki, H., Maker, P. D., Savage, C. M., Breitenbach, L. P., and Hurley, M. D.: FTIR
2 spectroscopic study of the mechanism for the gas-phase reaction between ozone and
3 tetramethylethylene, *J. Phys. Chem.*, 91, 941–946, 1987.

4 Novelli, A., Vereecken, L., Lelieveld, J., and Harder, H.: Direct observation of OH formation
5 from stabilised Criegee intermediates, *Phys. Chem. Chem. Phys.*, 16, 19941–19951, 2014.

6 Parrella, J. P., Jacob, D. J., Liang, Q., Zhang, Y., Mickley, L. J., Miller, B., Evans, M. J., Yang,
7 X., Pyle, J. A., Theys, N., and Van Roozendaal, M.: Tropospheric bromine chemistry:
8 implications for present and pre-industrial ozone and mercury, *Atmos. Chem. Phys.*, 12, 6723-
9 6740, 2012.

10 Paulot, F., Crounse, J. D., Kjaergaard, H. G., Kürten, A., Clair, J. M. S., Seinfeld, J. H., and
11 Wennberg, P. O.: Unexpected epoxide formation in the gas-phase photooxidation of isoprene,
12 *Science*, 325, 730-733, 2009a.

13 Paulot, F., Crounse, J. D., Kjaergaard, H. G., Kroll, J. H., Seinfeld, J. H., and Wennberg, P. O.:
14 Isoprene photooxidation: New insights into the production of acids and organic nitrates, *Atmos.*
15 *Chem. Phys.*, 9, 1479-1501, 2009b.

16 Paulson, S. E., Chung, M., Sen, A. D., and Orzechowska, G.: Measurement of OH radical
17 formation from the reaction of ozone with several biogenic alkenes, *Geophys. Res. Lett.*, 24,
18 3193–3196, 1997.

19 Peeters, J., Nguyen, T. L., and Vereecken, L.: HOx radical regeneration in the oxidation of
20 isoprene, *Phys. Chem. Chem. Phys.*, 11, 5935-5939, 2009.

21 Peeters, J., and Müller, J. F.: HOx radical regeneration in isoprene oxidation via peroxy
22 radical isomerisations. II: Experimental evidence and global impact, *Phys. Chem. Chem.*
23 *Phys.*, 12, 14227-14235, 2010.

24 Pöschl, U., and Shiraiwa, M.: Multiphase Chemistry at the Atmosphere-Biosphere Interface
25 Influencing Climate and Public Health in the Anthropocene, *Chem. Rev.*, 115, 4440–4475,
26 2015.

27 Rickard, A. R., Johnson, D., McGill, C. D., and Marston, G.: OH Yields in the Gas-Phase
28 reactions of Ozone with Alkenes, *J. Phys. Chem. A*, 103, 7656–7664, 1999.

29 Rossignol, S., Rio, C., Ustache, A., Fable, S., Nicolle, J., Mème, A., D’Anna, B., Nicolas, M.,
30 Leoz, E., and Chiappini, L.: The use of a housecleaning product in an indoor environment

Deleted: Peñuelas, J., and Staudt, M.: BVOCs and global change, *Trends Plant Sci.*, 15, 133–144, 2010.

1 leading to oxygenated polar compounds and SOA formation: Gas and particulate phase
2 chemical characterization, *Atmos. Environ.*, 75, 196-205, 2013.

3 Ryzhkov, A. B., and P. A. Ariya, A theoretical study of the reactions of parent and substituted
4 Criegee intermediates with water and the water dimer, *Phys. Chem. Chem. Phys.*, 6, 5042-5050,
5 2004.

6 Sarwar, G., and Corsi, R.: The effects of ozone/limonene reactions on indoor secondary organic
7 aerosols, *Atmos. Environ.*, 41, 959-973, 2007.

8 Saunders, S. M., Jenkin, M. E., Derwent, R. G., and Pilling, M. J.: Protocol for the development
9 of the Master Chemical Mechanism, MCM v3 (Part A): Tropospheric degradation of non-
10 aromatic volatile organic compounds, *Atmos. Chem. Phys.*, 3, 161-180, 2003.

11 Shallcross, D. E., Taatjes, C. A., and Percival, C. J.: Criegee intermediates in the indoor
12 environment: new insights, *Indoor Air*, 24, 495-502, 2014.

13 Sheps, L., Scully, A. M., and Au, K.: UV absorption probing of the conformer-dependent
14 reactivity of a Criegee intermediate CH_3CHOO *Phys. Chem. Chem. Phys.*, 16, 26701-26706,
15 2014.

16 [Sheps, L., Rotavera, B., Eskola, A. J., Osborn, D. L., Taatjes, C. A., Au, K., Shallcross, D. E.,
17 Khan, M. A. H., and Percival, C. J.: The reaction of Criegee intermediate \$\text{CH}_2\text{OO}\$ with water
18 dimer: primary products and atmospheric impact, *Phys. Chem. Chem. Phys.*, 19, 21970-21979,
19 2017.](#)

20 Sindelarova, K., Granier, C., Bouarar, I., Guenther, A., Tilmes, S., Stavrou, T., Müller, J.-F.,
21 Kuhn, U., Stefani, P., and Knorr, W.: Global data set of biogenic VOC emissions calculated by
22 the MEGAN model over the last 30 years, *Atmos. Chem. Phys.*, 14, 9317-9341, 2014.

23 Singer, B. C., Coleman, B. K., Destailats, H., Hodgson, A. T., Lunden, M. M., Weschler, C.
24 J., and Nazaroff, W. W.: Indoor secondary pollutants from cleaning product and air freshener
25 use in the presence of ozone, *Atmos. Environ.*, 40, 6696-6710, 2006a.

26 Singer, B. C., Destailats, H., Hodgson, A. T., and Nazaroff, W. M.: Cleaning products and air
27 fresheners: emissions and resulting concentrations of glycol ethers and terpenoids, *Indoor Air*,
28 16, 179-191, 2006b.

29 Sipilä, M., Jokinen, T., Berndt, T., Richters, S., Makkonen, R., Donahue, N. M.,
30 Mauldin III, R. L., Kurtén, T., Paasonen, P., Sarnela, N., Ehn, M., Junninen, H., Rissanen, M. P.,

1 Thornton, J., Stratmann, F., Herrmann, H., Worsnop, D. R., Kulmala, M., Kerminen, V.-M.,
2 and Petäjä, T.: Reactivity of stabilized Criegee intermediates (sCIs) from isoprene and
3 monoterpene ozonolysis toward SO₂ and organic acids, *Atmos. Chem. Phys.*, 14, 12143-12153,
4 2014.

5 Smith, M. C., Chao, W., Takahashi, K., Boering, K. A., and Lin, J. J. -M.: Unimolecular
6 Decomposition Rate of the Criegee Intermediate (CH₃)₂COO Measured Directly with UV
7 Absorption Spectroscopy, *J. Phys. Chem. A*, doi: 10.1021/acs.jpca.5b12124, 2016.

8 Stone, D., Blitz, M., Daubney, L., Howes, N. U. M., and Seakins, P.: Kinetics of CH₂OO
9 reactions with SO₂, NO₂, NO, H₂O, and CH₃CHO as a function of pressure, *Phys. Chem. Chem.*
10 *Phys.*, 16, 1139-1149, 2014.

11 Su, Y. -T., Lin, H. -Y., Putikam, R., Matsui, H., Lin, M. C., and Lee, Y. -P.: Extremely rapid
12 self-reaction of the simplest Criegee intermediate CH₂OO and its implications in atmospheric
13 chemistry, *Nature Chemistry*, 6, 477-483, 2014.

14 Taatjes, C. A., Welz, O., Eskola, A. J., Savee, J. D., Osborn, D. L., Lee, E. P. F., Dyke, J. M.,
15 Mok, D. W. K., Shallcross, D. E., and Percival, C. J.: Direct measurements of Criegee
16 intermediate (CH₂OO) formed by reaction of CH₂I with O₂, *Phys. Chem. Chem. Phys.*, 14,
17 10391-10400, 2012.

18 Taatjes, C. A., Welz, O., Eskola, A. J., Savee, J. D., Scheer, A. M., Shallcross, D. E., Rotavera,
19 B., Lee, E. P. F., Dyke, J. M., Mok, D. K. W., Osborn, D. L., and Percival, C. J.: Direct
20 Measurements of Conformer-Dependent Reactivity of the Criegee Intermediate CH₃CHOO,
21 *Science*, 340, 177-180, 2013.

22 Taatjes, C. A., Shallcross, D. E., and Percival, C. J.: Research frontiers in the chemistry of
23 Criegee intermediates and tropospheric ozonolysis, *Phys. Chem. Chem. Phys.*, 16, 1704-1718,
24 2014.

25 Taipale, R., Sarnela, N., Rissanen, M., Junninen, H., Rantala, P., Korhonen, F., Siivola, E.,
26 Berndt, T., Kulmala, M., Mauldin, R.L. III, Petäjä, T., Sipilä, M.: New instrument for measuring
27 atmospheric concentrations of non-OH oxidants of SO₂, *Bor. Env. Res.*, 19 (suppl. B), 55-70,
28 2014.

29 Truhlar, D. G., Garrett, B. C. and Klippenstein, S. J.: Current Status of Transition-State Theory,
30 *J. Phys. Chem.*, 100, 12771-12800, 1996.

- 1 Vereecken, L. and Peeters, J.: The 1,5-H-shift in 1-butoxy: A case study in the rigorous
2 implementation of transition state theory for a multirotamer system, *J. Chem. Phys.*, 119, 5159-
3 5170, 2003.
- 4 Vereecken, L., and Francisco, J. S.: Theoretical studies of atmospheric reaction mechanisms in
5 the troposphere, *Chem. Soc. Rev.*, 41, 6259-6293, 2012.
- 6 Vereecken, L., Harder, H., and Novelli, A.: The reaction of Criegee intermediates with NO,
7 RO₂, and SO₂, and their fate in the atmosphere, *Phys. Chem. Chem. Phys.*, 14, 14682–14695,
8 2012.
- 9 Vereecken, L., Harder, H., and Novelli, A.: The reactions of Criegee intermediates with
10 alkenes, ozone and carbonyl oxides, *Phys. Chem. Chem. Phys.*, 16, 4039–4049, 2014.
- 11 Vereecken, L., Rickard, A. R., Newland, M. J., and Bloss, W. J.: Theoretical study of the
12 reactions of Criegee intermediates with ozone, alkylhydroperoxides, and carbon monoxide,
13 *Phys. Chem. Chem. Phys.*, 17, 23847–23858, 2015.
- 14 Vereecken, L., and Nguyen, H. M. T.: Theoretical Study of the Reaction of Carbonyl Oxide
15 with Nitrogen Dioxide: CH₂OO + NO₂, *Int. J. Chem. Kinet.*, 49, 752-760, 2017.
- 16 Vereecken, L.: The Reaction of Criegee Intermediates with Acids and Enols, *Phys. Chem.*
17 *Chem. Phys.*, DOI: 10.1039/C7CP05132H, 2017.
- 18 Vereecken, L., Novelli, A., and Taraborrelli, D.: Unimolecular decay strongly limits
19 concentration of Criegee intermediates in the atmosphere, [Phys. Chem. Chem. Phys.](#), 19,
20 [31599–31612](#), doi:10.1039/C7CP05541B, 2017.
- 21 Wang, L., and Wang, L.: Mechanism of gas-phase ozonolysis of sabinene in the atmosphere,
22 *Phys. Chem. Chem. Phys.*, doi: 10.1039/c7cp03216a, 2017.
- 23 Wei, W., Zheng, R., Pan, Y., Wu, Y., Yang, F., and Hong, S.: Ozone Dissociation to Oxygen
24 Affected by Criegee Intermediate, *J. Phys. Chem. A*, 118, 1644–1650, 2014.
- 25 Wei, W. -M., Yang, X., Zheng, R. -H., Qin, Y. -D., Wu, Y. -K., Yang, F.: Theoretical studies
26 on the reactions of the simplest Criegee intermediate CH₂OO with CH₃CHO, *Comp. Theor.*
27 *Chem.*, 1074, 142-149, 2015.
- 28 Welz, O., Eskola, A. J., Sheps, L., Rotavera, B., Savee, J. D., Scheer, A. M., Osborn, D. L.,
29 Lowe, D., Murray Booth, A., Xiao, P., Anwar H., Khan, M., Percival, C. J., Shallcross, D. E.,
30 and Taatjes, C. A.: Rate coefficients of C1 and C2 Criegee intermediate reactions with formic

Formatted: Normal

Deleted: .,

Deleted: Manuscript in preparation

1 and acetic acid near the collision limit: direct kinetics measurements and atmospheric
 2 implications, *Angew. Chem. Int. Ed. Engl.*, 53, 4547–4750, 2014.

3 Welz, O., Savee, J. D., Osborn, D. L., Vasu, S. S., Percival, C. J., Shallcross, D. E., and Taatjes,
 4 C. A.: Direct Kinetic Measurements of Criegee Intermediate (CH₂OO) Formed by Reaction of
 5 CH₂I with O₂, *Science*, 335, 204–207, 2012.

6 Winterhalter, R., Neeb, P., Grossmann, D., Kolloff, A., Horie, O., and Moortgat, G.: Products
 7 and Mechanism of the Gas Phase Reaction of Ozone with β-pinene, *J. Atmos. Chem.*, 35, 165-
 8 197, 2000.

9 Yao, L., Ma, Y., Wang, L., Zheng, J., Khalizov, A., Chen, M., Zhou, Y., Qi, L., and Cui, F.:
 10 Role of stabilized Criegee Intermediate in secondary organic aerosol formation from the
 11 ozonolysis of α-cedrene, *Atmos. Environ.*, 94, 448-457, 2014.

12 Zhang, D., and Zhang, R.: Ozonolysis of α-pinene and β-pinene: Kinetics and mechanism, *J.*
 13 *Chem. Phys.*, 122, 114308, 2005.

14 Zhang, J., Huff Hartz, K. E., Pandis, S. N., and Donahue, N. M.: Secondary Organic Aerosol
 15 Formation from Limonene Ozonolysis: Homogeneous and Heterogeneous Influences as a
 16 Function of NO_x, *J. Phys. Chem. A*, 110, 11053-11063, 2006.

17 Zhou, L., Gierens, R., Sogachev, A., Mogensen, D., Ortega, J., Smith, J. N., Harley, P. C.,
 18 Prenni, A. J., Levin, E. J. T., Turnipseed, A., Rusanen, A., Smolander, S., Guenther, A. B.,
 19 Kulmala, M., Karl, T., and Boy, M.: Contribution from biogenic organic compounds to particle
 20 growth during the 2010 BEACHON-ROCS campaign in a Colorado temperate needle leaf
 21 forest, *Atmos. Chem. Phys. Discuss.*, 15, 9033-9075, doi:10.5194/acpd-15-9033-2015, 2015.

22 Table 1. Monoterpene SCI yields derived in this work and reported in the literature.

Φ_{SCI}	Reference	Notes	Methodology
<i>α-pinene</i>			
0.19 (± 0.01)	This work		SO ₂ loss
0.15 (± 0.07)	Sipilä et al. (2014)		Formation of H ₂ SO ₄
0.22	Taipale et al. (2014) (personal comm. Berndt)		
0.125 (± 0.04)	Hatakeyama et al. (1984)		Formation of H ₂ SO ₄
0.20	MCMv3.3.1 ^a		

Deleted: . [2]

Formatted Table

<i>β-pinene</i>			
0.60 (± 0.03)	This work		SO ₂ loss
0.46	Ahrens et al. (2014)	φ _{C9-SCI} : 0.36 φ _{CH2OO} : 0.10	FTIR detection
0.25	MCMv3.3.1 ^a	φ _{C9-SCI} : 0.102 φ _{CH2OO} : 0.148	
0.42	Nguyen et al. (2009)	φ _{C9-SCI} : 0.37 φ _{CH2OO} : 0.05	Theoretical
0.51	Winterhalter et al. (2000)	φ _{C9-SCI} : 0.35 φ _{CH2OO} : 0.16	Change in nopinone yields <i>f</i> ([H ₂ O])
0.44	Kotzias et al. (1990)		Formation of H ₂ SO ₄
0.25	Hatakeyama et al. (1984)		Formation of H ₂ SO ₄
0.30	Zhang and Zhang (2005)	φ _{C9-SCI} : 0.22 φ _{CH2OO} : 0.08	
> 0.27	Ma and Marston (2008)	φ _{C9-SCI} : 0.27 φ _{CH2OO} : 0.16 ^a φ _{CH2OO} : 0.06 ^b	Change in nopinone yields <i>f</i> ([H ₂ O])
0.27	Hasson et al. (2001)		Change in nopinone yields <i>f</i> ([H ₂ O])
<i>Limonene</i>			
0.23 (± 0.01)	This work		SO ₂ loss
0.27 (± 0.12)	Sipilä et al. (2014)		Formation of H ₂ SO ₄
0.34	Leungsakul et al. (2005)	φ _{C10-SCI} : 0.26 φ _{Cl-x} : 0.04 φ _{CH2OO} : 0.05	Measurement of stable particle and gas-phase products
0.135	MCMv3.3.1 ^a		

1 Uncertainty ranges (± 2σ, parentheses) indicate combined precision and systematic measurement error
2 components for this work, and are given as stated for literature studies. All referenced experimental studies
3 produced SCI from MT + O₃ and were conducted between 700 and 760 Torr. ^a <http://mcm.leeds.ac.uk/MCM/>
4 (Jenkin et al., 2015).

5 ^a assuming 100 % stabilisation

6 ^b assuming 40 % stabilisation

1 Table 2. Monoterpene derived SCI relative and absolute^a rate constants derived in this work.

SCI	$10^5 k_3/k_2$	$10^{15} k_3$ ($\text{cm}^3 \text{s}^{-1}$)	$10^{-12} k_d/k_2$ (cm^{-3})	k_d (s^{-1})
<i>α-pinene</i>				
SCI-A	> 140 (± 34)	> 310 (± 75) ^a		
SCI-B			< 8.2 (± 1.5)	< 240 (± 44) ^c
<i>β-pinene</i>				
SCI-A	> 10 (± 2.7)	> 4 (± 1) ^b		
SCI-B			< 6.0 (± 1.3)	< 170 (± 38) ^c
<i>Limonene</i>				
SCI-A	< 3.5 (± 0.2)	< 7.7 (± 0.6) ^a		
SCI-B			> 4.5 (± 0.1)	> 130 (± 3) ^c

2 Uncertainty ranges ($\pm 2\sigma$, parentheses) indicate combined precision and systematic measurement error
 3 components. ^a Scaled to an absolute value using $k_2(\text{anti-CH}_3\text{CHOO}) = 2.2 \times 10^{-10} \text{ cm}^3 \text{ s}^{-1}$ (Sheps et al., 2014); ^b
 4 Scaled to an absolute value using $k_2(\text{anti-CH}_3\text{CHOO}) = 4 \times 10^{-11} \text{ cm}^3 \text{ s}^{-1}$ (Ahrens et al., 2014); ^c Scaled using $k_2(\text{syn-}$
 5 $\text{CH}_3\text{CHOO}) = 2.9 \times 10^{-11} \text{ cm}^3 \text{ s}^{-1}$ (Sheps et al., 2014).

6
7
8
9
10
11
12
13

Formatted Table

1 Table 3. Unimolecular reactions for the CI derived from α -pinene, β -pinene, and *d*-limonene,
 2 as derived by Vereecken et al. (2017). Barrier heights (kcal mol⁻¹) listed estimate post-CCSD(T)
 3 energies.

Carbonyl oxide	Reaction	E_b	$k(298K) / s^{-1}$
<i>α-pinene</i>			
CI-1a	1,4-H-migration	15.8	600
	SOZ-formation	15.6	5×10^{-2}
CI-1b	1,3-ring closure	21.6	1×10^{-3}
	1,3-H-migration	29.0	1×10^{-6}
CI-2a	1,4-H-migration	16.3	250
	1,3-ring closure	20.8	6×10^{-3}
CI-2b	1,4-H-migration	17.0	60
	SOZ-formation	13.5	8
	Ring closure	19.9	3×10^{-2}
<i>β-pinene</i>			
CI-3	1,4-H-migration	15.7	375
	1,3-ring closure	21.1	2×10^{-3}
CI-4	1,3-ring closure	17.2	2.0
	Ring opening	23.6	(Slow, Nguyen et al. 2009a)
CH ₂ OO	1,4-H-migration	24.9	(Slow, Nguyen et al. 2009a)
	1,3-ring closure	19.0	0.3
	1,3-H-migration	30.7	1×10^{-7}
<i>Limonene^a</i>			
CI-5a	1,4-H-migration	SAR	200 ^a
CI-5b	1,3-ring closure	SAR	75 ^a
CI-6a	1,4-H-migration	SAR	430 ^a
CI-6b	1,4-H-migration	SAR	700 ^a
CI-7a	1,4-H-migration	SAR	15
CI-7b	1,4-H-migration	SAR	600

4 ^a Formation of secondary ozonides (SOZ) is not included, and could be the dominant unimolecular loss.

5

6

Formatted Table

1 Table 4. Rate coefficients ($\text{cm}^3 \text{ molecule}^{-1} \text{ s}^{-1}$) for the reaction of CI with H_2O and $(\text{H}_2\text{O})_2$ as
 2 predicted by Vereecken et al. (2017). Values are based on explicit CCSD(T)/aug-cc-
 3 pVTZ//M06-2X/aug-cc-pVTZ calculations and multi-conformer TST, including empirical
 4 corrections to reference experimental data, except for limonene-derived CI where the values
 5 are predicted using a structure-activity relationship. The rate coefficients for CH_2OO ,
 6 CH_3CHOO , and $(\text{CH}_3)_2\text{COO}$ are within a factor of 4 of evaluated literature data (Vereecken et
 7 al., 2017).

Carbonyl oxide	$k(298\text{K}) \text{H}_2\text{O}$	$k(298\text{K}) (\text{H}_2\text{O})_2$
CH_2OO	8.7×10^{-16}	1.4×10^{-12}
<i>syn</i> - CH_3CHOO	6.7×10^{-19}	2.1×10^{-15}
<i>anti</i> - CH_3CHOO	2.3×10^{-14}	2.7×10^{-11}
$(\text{CH}_3)_2\text{COO}$	7.5×10^{-18}	1.8×10^{-14}
<i>α-pinene</i>		
CI-1a	1.3×10^{-18}	2.9×10^{-15}
CI-1b	1.5×10^{-14}	1.7×10^{-11}
CI-2a	1.0×10^{-18}	2.5×10^{-15}
CI-2b	2.4×10^{-19}	7.0×10^{-16}
<i>β-pinene</i>		
CI-3	1.7×10^{-18}	4.3×10^{-15}
CI-4	4.2×10^{-16}	6.4×10^{-13}
<i>Limonene</i>		
CI-5a	1.5×10^{-18}	4.3×10^{-15}
CI-5b	1.5×10^{-14}	1.7×10^{-11}
CI-6a	9.1×10^{-18}	2.1×10^{-14}
CI-6b	1.5×10^{-17}	3.2×10^{-14}
CI-7a	9.7×10^{-18}	1.9×10^{-14}
CI-7b	4.3×10^{-18}	1.1×10^{-14}

Formatted Table

8

9

1 Table 5. Kinetic parameters used in the global modelling study.

SCI	ϕ_{SCI}	$10^{15} k_3$ ($\text{cm}^3 \text{s}^{-1}$)	$10^{11} k_2^a$ ($\text{cm}^3 \text{s}^{-1}$)	k_d (s^{-1})
<i>α-pinene</i>				
SCI-A	0.08	310	22	-
SCI-B	0.11	-	2.9	240
<i>β-pinene</i>				
SCI-A	0.25	4	4	-
SCI-B	0.35	-	2.9	170
<i>Limonene</i>				
SCI-A	0.05	7.7	22	-
SCI-B	0.18	-	2.9	130
<i>Myrcene</i>				
SCI-B	0.30	-	13 ^b	400 ^c
<i>Ocimene</i>				
SCI-B	0.30	-	13 ^b	400 ^c
<i>Sabinene</i>^d				
SCI-A	0.25	4	4	-
SCI-B	0.35	-	2.9	170
<i>3-carene</i>^e				
SCI-A	0.08	310	22	-
SCI-B	0.11	-	2.9	240

Formatted Table

Deleted: 819°

Deleted: 819°

Deleted: Newland et al. (2015) (scaled to $k_2(\text{SCI-B}+\text{SO}_2)$ from Huang et al. (2015)

2 ^a $k_2(\text{SCI-A}+\text{SO}_2)$ from ($\text{SO}_2+\text{anti-CH}_3\text{CHO}$) - Sheps et al. (2014); $k_2(\text{SCI-B}+\text{SO}_2)$ from ($\text{SO}_2+\text{syn-CH}_3\text{CHO}$)

3 - Sheps et al. (2014) unless otherwise stated

4 ^b $k_2(\text{SCI-B}+\text{SO}_2)$ from ($\text{SO}_2+\text{anti}-(\text{CH}_3)_2\text{COO}$) - Huang et al. (2015)

5 ^c Temp dependent $k_d(\text{SCI-B})$ taken from JUPAC recommendation (2017)

6 ^d Kinetics based on β -pinene

7 ^e Kinetics based on α -pinene

8

1 Table 6. Monoterpene contribution to [SCI] and SO₂ oxidation in the surface layer of the
 2 model simulation.

Monoterpene	Annual emissions ^a (Tg C)	% contribution to [SCI-A]	% contribution to [SCI-B]	% contribution to SO ₂ oxidation
α -pinene	35.4	0.5	15	5.8
β -pinene	16.9	74	43	54
limonene	9.2	3.5	13	6.0
myrcene	3.1	0.0	2.7	9.0
trans- β -ocimene	14.1	0.0	11	20
sabinene	7.9	22	13	3.8
3-carene	6.4	0.0	2.5	1.3

3 ^a From MEGAN v2.1 (Guenther et al., 2012)
 4

Formatted Table

Deleted: 16

Deleted: 6.9

Deleted: 46

Deleted: 65

Deleted: 14

Deleted: 7.2

Deleted: 1.

Deleted: 4.5

Deleted: 5.4

Deleted: 11

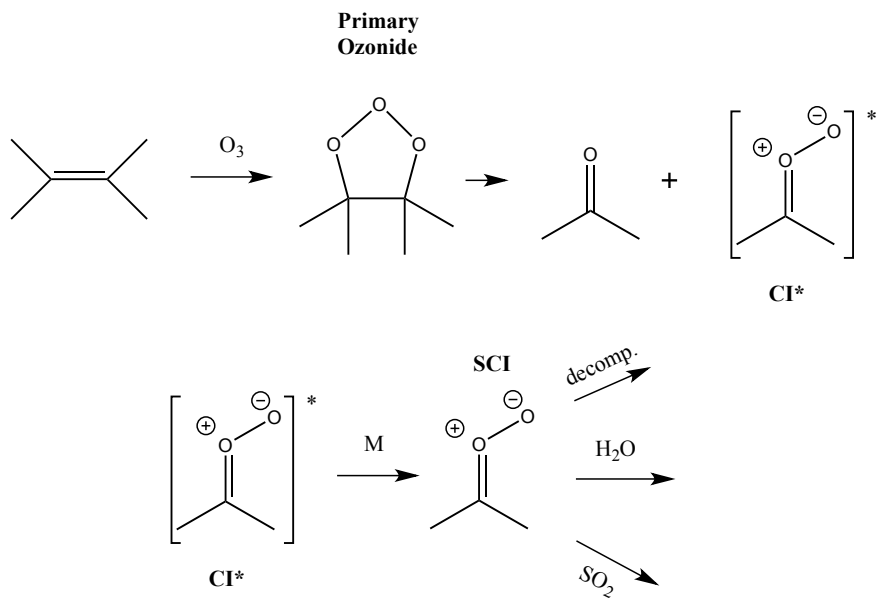
Deleted: 14

Deleted: 4.5

Deleted: 7

Deleted: 6

1



2

3 Scheme 1. Simplified generic mechanism for the reaction of Criegee Intermediates (CIs)
4 formed from alkene ozonolysis.

5

6

7

8

9

10

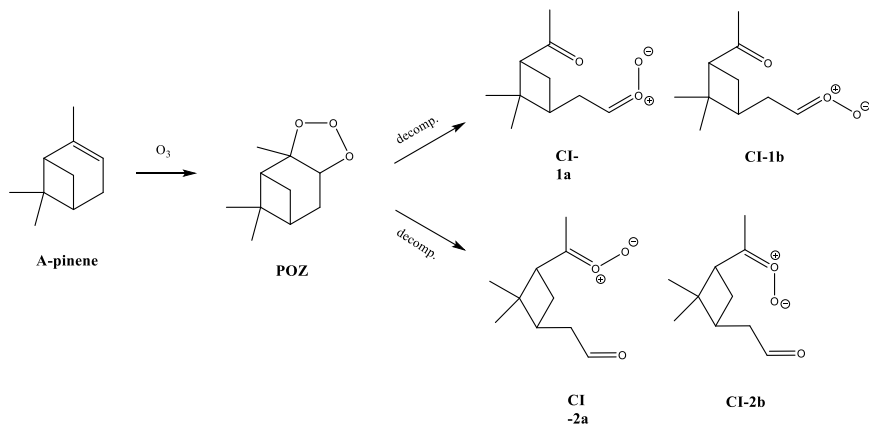
11

12

13

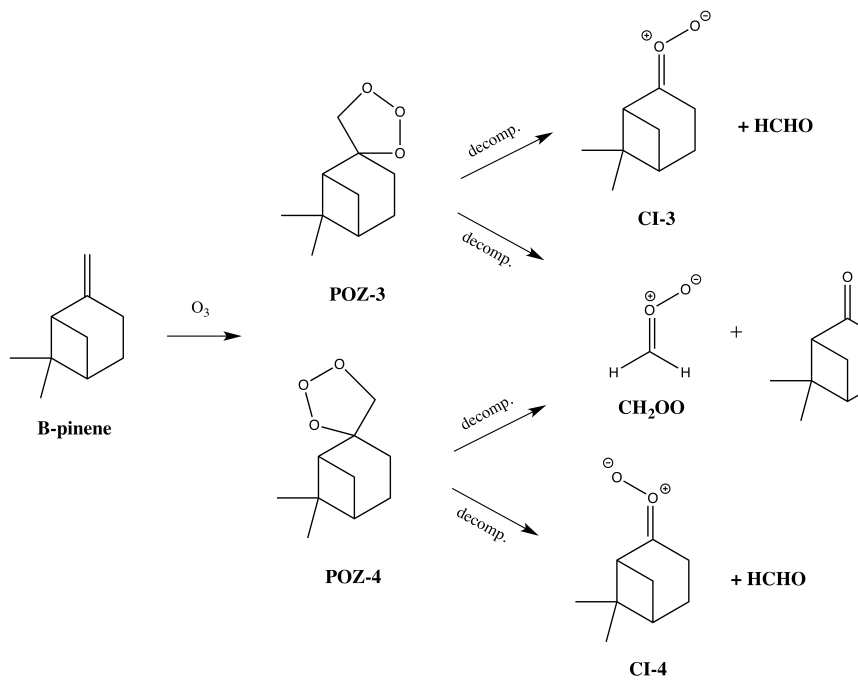
14

15



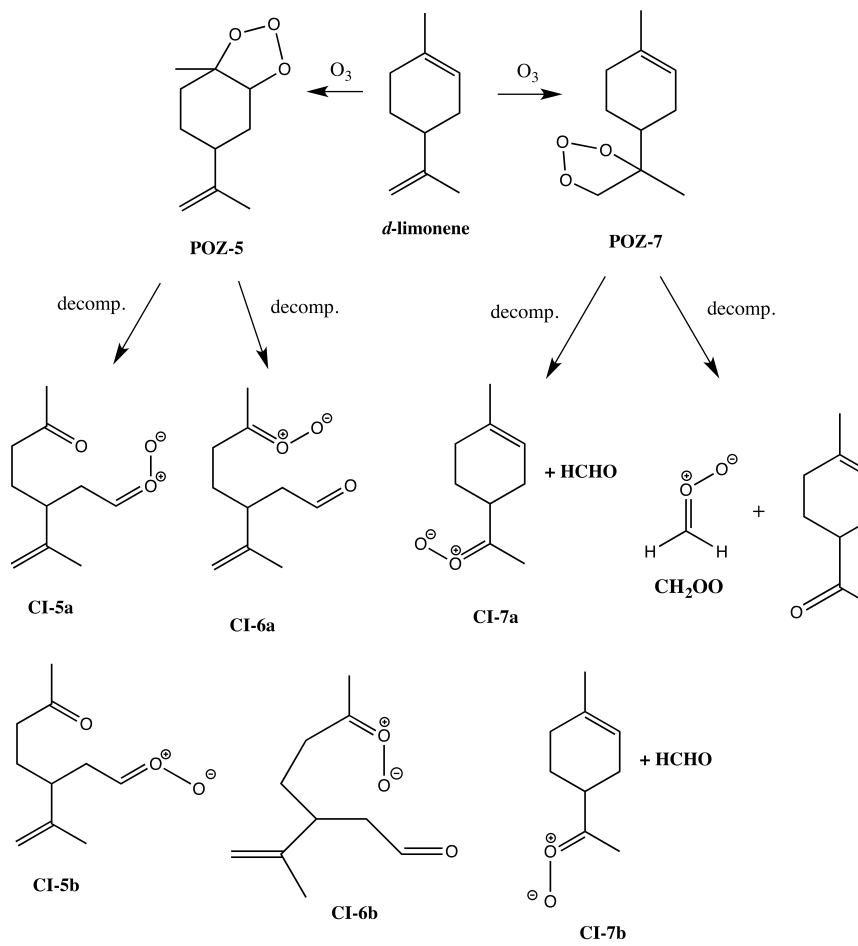
1
2
3
4
5
6
7
8
9
10

Scheme 2. Mechanism of formation of the two Criegee Intermediates (CIs) from α -pinene ozonolysis.



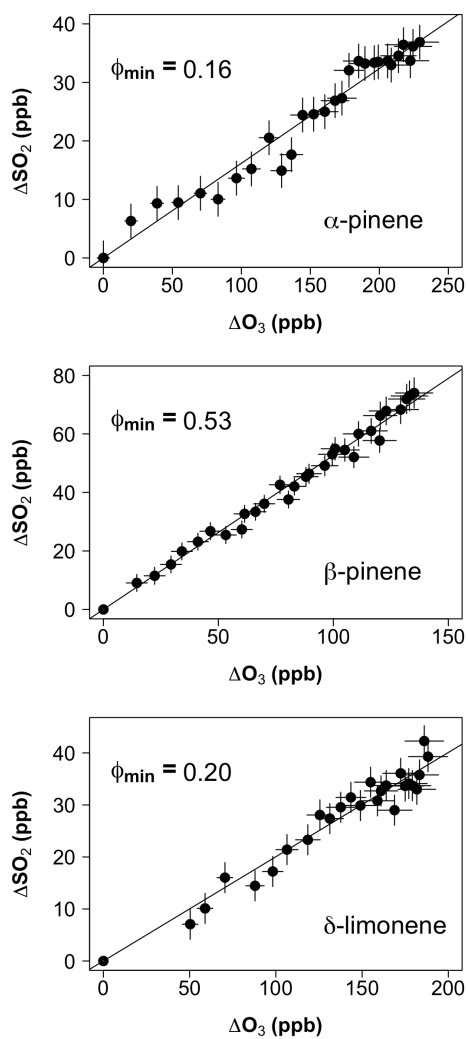
1
2

3 Scheme 3. Mechanism of formation of the three Criegee Intermediates (CIs) from β -pinene
4 ozonolysis.

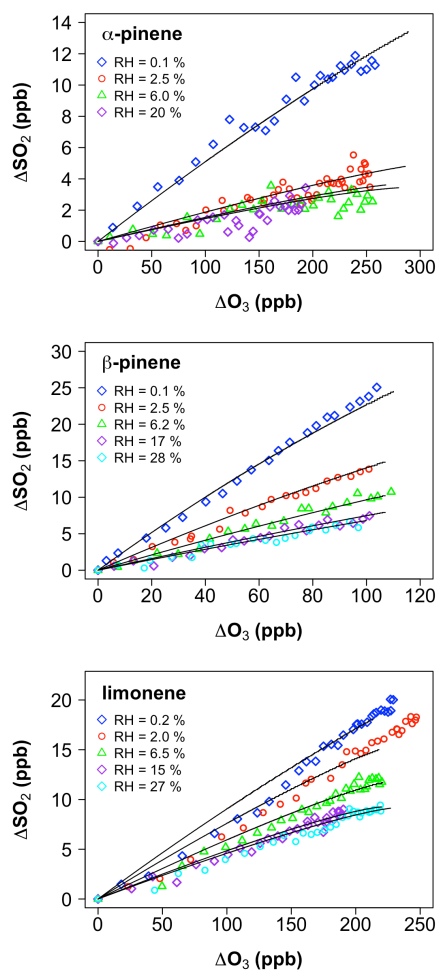


1
2
3
4
5

Scheme 4. Mechanism of formation of the four Criegee Intermediates (CIs) from limonene ozonolysis.

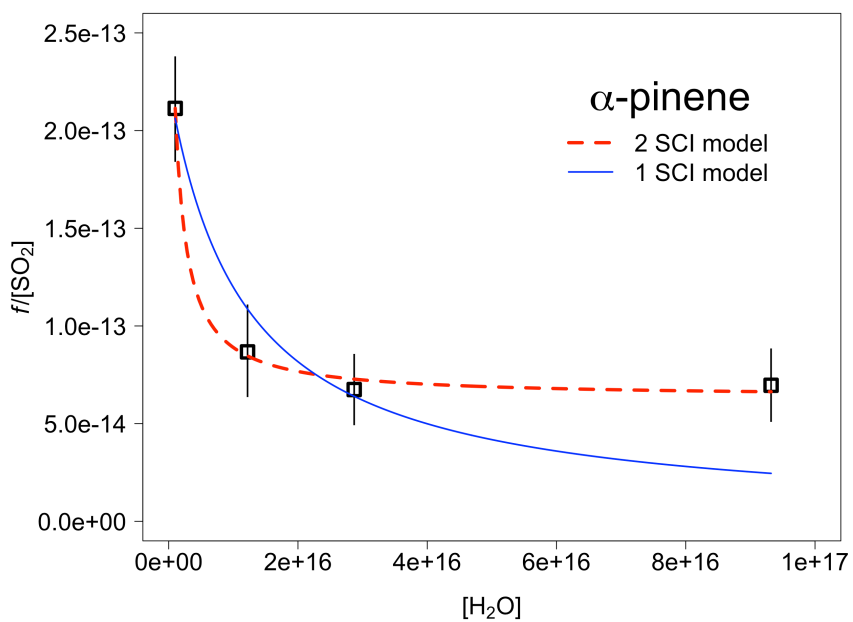


1
2 Figure 1. ΔSO_2 vs. ΔO_3 during excess SO_2 experiments ($[\text{H}_2\text{O}] < 5 \times 10^{15} \text{ cm}^{-3}$). The gradient
3 determines the minimum SCI yield (ϕ_{\min}).
4



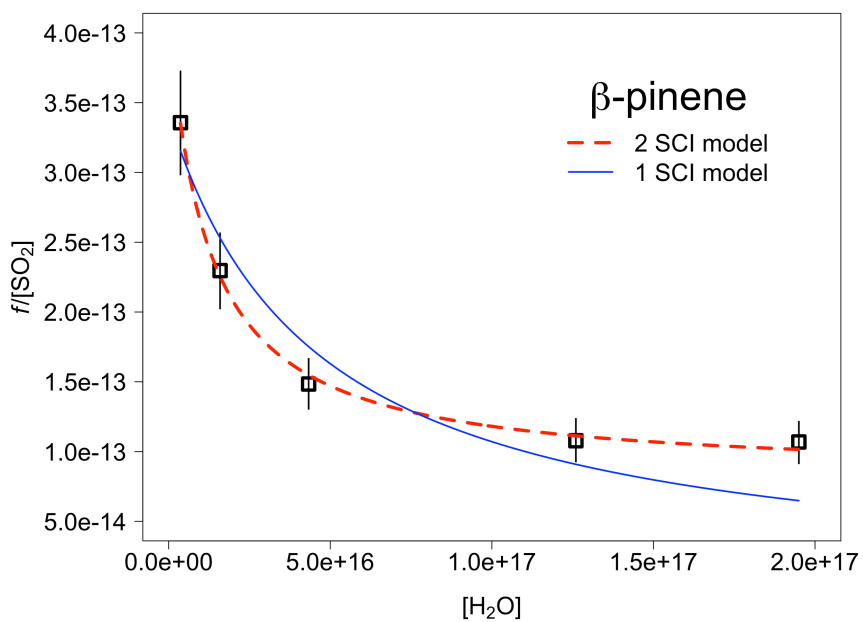
1
 2 Figure 2. Cumulative consumption of SO₂ as a function of cumulative consumption of O₃, ΔSO₂
 3 versus ΔO₃, for the ozonolysis of α-pinene, β-pinene and limonene in the presence of SO₂ at a
 4 range of water vapour concentrations, from $1 \times 10^{15} \text{ cm}^{-3}$ to $1.9 \times 10^{17} \text{ cm}^{-3}$. Symbols are
 5 experimental data, corrected for chamber dilution. Lines are smoothed fits to the experimental
 6 data.

7

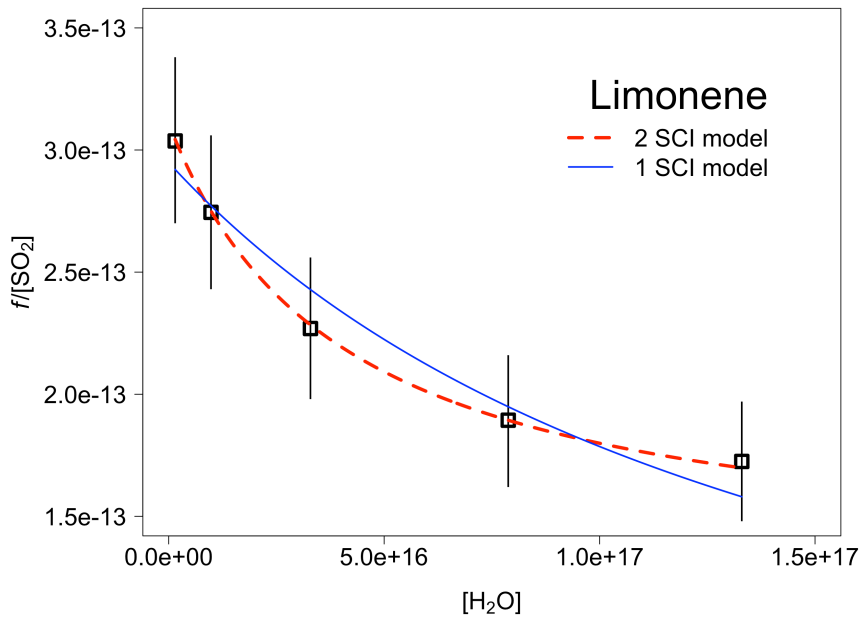


1
 2 Figure 3. Application of a 2 SCI model fit (Equation E4) and a single SCI model fit (Equation
 3 E1) to the measured values (open squares) of $f/[\text{SO}_2]$ for α -pinene. From the fit we derive
 4 relative rate constants for reaction of the α -pinene derived SCI, SCI-A and SCI-B with H_2O
 5 (k_3/k_2) and decomposition ($(k_d+L)/k_2$) assuming that $\gamma^A = 0.40$ and $\gamma^B = 0.60$.

6
 7
 8
 9
 10

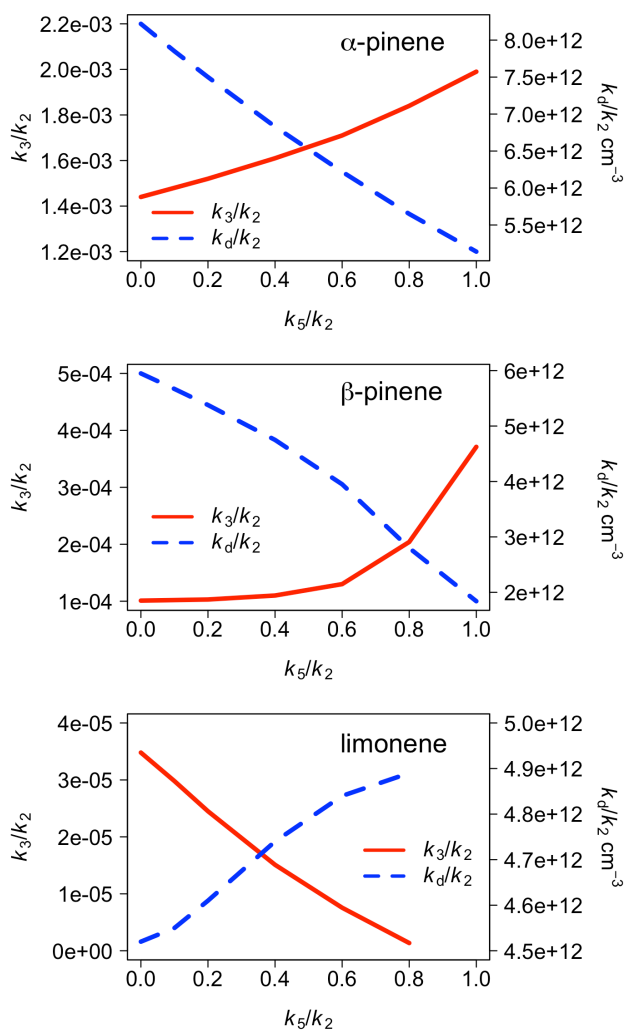


1
 2 Figure 4. Application of a 2 SCI model fit (Equation E4) and a single SCI model fit (Equation
 3 E1) to the measured values (open squares) of $f/[\text{SO}_2]$ for β -pinene. From the fit we derive
 4 relative rate constants for reaction of the β -pinene derived SCI, SCI-A and SCI-B with H_2O
 5 (k_3/k_2) and decomposition ($(k_d+L)/k_2$) assuming that $\gamma^A = 0.41$ and $\gamma^B = 0.59$.

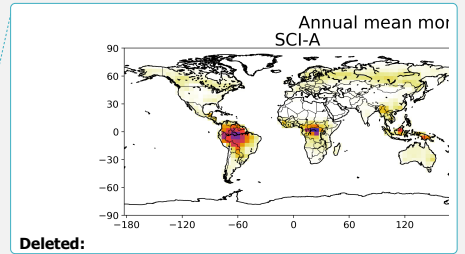
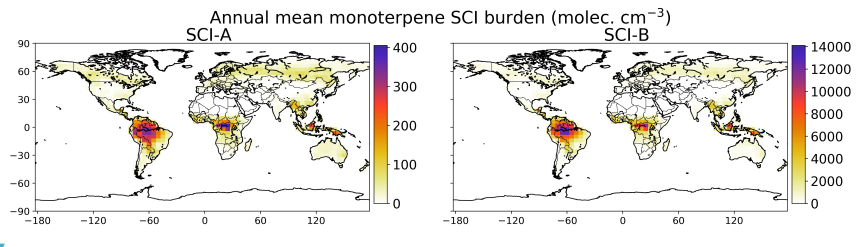


1
2
3
4
5
6
7
8
9
10
11
12
13

Figure 5. Application of a 2 SCI model fit (Equation E4) and a single SCI model fit (Equation E1) to the measured values (open squares) of $f/[\text{SO}_2]$ for limonene. From the fit we derive relative rate constants for reaction of the limonene derived SCI, SCI-A and SCI-B with H_2O (k_3/k_2) and decomposition ($(k_d+L)/k_2$) assuming that $\gamma^A = 0.22$ and $\gamma^B = 0.78$.

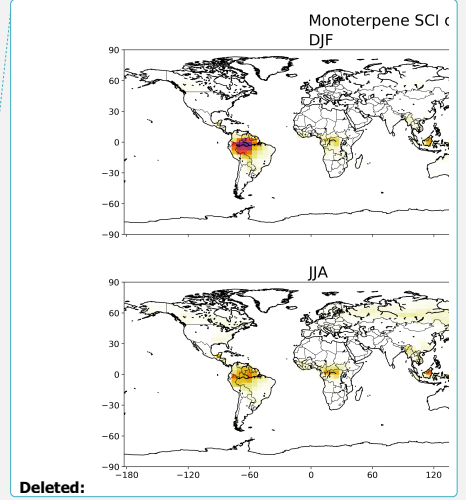
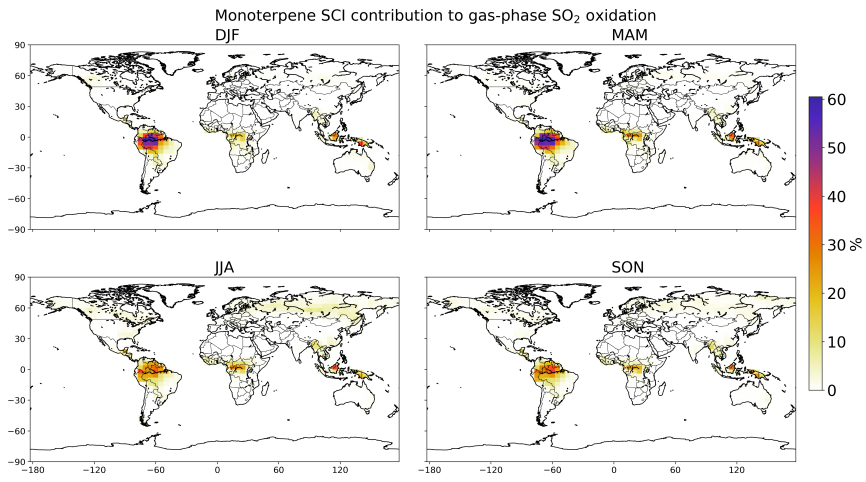


1
 2 Figure 6. Variation of k_3/k_2 ($k(\text{SCI-A}+\text{H}_2\text{O})/k(\text{SCI-A}+\text{SO}_2)$) and k_d ($k(\text{SCI-B unimol.})/k(\text{SCI-B}+\text{SO}_2)$) as a function of the ratio k_5/k_2 ($k(\text{SCI+acid})/k(\text{SCI}+\text{SO}_2)$), derived from least squares
 3 fit of Equation E4 to measurements shown in Figures 3 -5 for α -pinene, β -pinene and limonene
 4 respectively.
 5
 6
 7



1
2
3
4
5
6
7
8

Figure 7. Annual mean monoterpene SCI-A and SCI-B concentrations (cm^{-3}) in the surface layer of the GEOS-Chem simulation.



1
2 Figure 8. Seasonal SO₂ oxidation by monoterpene SCI as percentage of total gas-phase SO₂
3 oxidation in the surface layer.
4
5

Discussion and Atmospheric Implications

Monoterpene ozonolysis produces a diverse range of SCIs, with contrasting fates in the atmosphere, dominated by unimolecular reaction or reaction with water vapour, but which may still affect atmospheric SO₂ processing. Monoterpene-derived SCI have the potential to make a significant contribution to gas-phase SO₂ oxidation in specific local (i.e. forested) environments, of up to 50 % at certain times of year - amplifying sulfate aerosol formation, reducing the atmospheric lifetime and hence geographic distribution of SO₂, however the results presented here show that their impact upon annual SO₂ oxidation globally is modest. The results presented here demonstrate that it is important that monoterpene ozonolysis reactions are considered to produce at least two different SCI species if their chemistry is to be adequately represented in global models. This is because even a 'moderate' reaction rate with water would be a dominant sink of an SCI with the averaged properties of SCI-A and SCI-B.

SCI concentrations are expected to vary greatly depending on the local environment and time of year, *e.g.* monoterpene abundance may be considerably higher (and with a different reactive mix of alkenes giving a range of structurally diverse SCI) in a forested environment, compared to a rural background. Furthermore, biogenic isoprene and monoterpene emissions are strongly temperature dependent, hence are predicted to change significantly in the future as a response to a changing climate and other environmental conditions (Peñuelas and Staudt, 2010).

This study shows that the ozonolysis of monoterpenes may contribute to significant SCI concentrations in forested areas. Another group of compounds produced by forests that may also have the potential to be a significant source of SCI are sesquiterpenes (C₁₅H₂₄). Although generally present at low mixing ratios, this is due to their short atmospheric lifetimes caused by their rapid reaction rates with ozone. The flux through the alkene-ozone reaction for fast reacting monoterpenes and sesquiterpenes is often higher than for monoterpenes with high mixing ratios but low removal rates, *e.g.* α-pinene and β-pinene. Ozonolysis of sesquiterpenes has been shown to have very high SCI yields (Beck et al., 2011; Yao et al., 2014) and these SCI have been shown to react with SCI scavengers (*e.g.* SO₂, H₂O etc.) in a similar way to smaller SCI (Yao et al., 2014). It has been predicted that SCI from sesquiterpenes may have a high degree of secondary ozonide formation (Chuong et al., 2004) but experimental work has shown very different results for structurally different sesquiterpenes studied (Beck et al., 2011; Yao et al., 2014) hence this is highly uncertain, as is the fate of the SOZ once formed. Therefore, these have the potential to be another significant source of SCI.

